Journal of Sedimentary Research

Journal of Sedimentary Research, 2007, v. 77, 826–842
Research Article
DOI: 10.2110/jsr.2007.079

PALEOENVIRONMENTAL AND CARBON-OXYGEN ISOTOPE RECORD OF MIDDLE CAMBRIAN CARBONATES (LA LAJA FORMATION) IN THE ARGENTINE PRECORDILLERA

FERNANDO J. GOMEZ,[1] NEIL OGLE,[2] RICARDO A. ASTINI,[1] AND ROBERT M. KALIN[2]
[1]*Laboratorio de Análisis de Cuencas, CICTERRA-CONICET, Facultad de Ciencias Exactas, Físicas y Naturales, Universidad Nacional de Córdoba, Avenida Vélez Sarsfield 1611, X5016GCA, Córdoba, Argentina*
[2]*Environmental Engineering Research Center, School of Planning, Architecture and Civil Engineering, The Queen's University of Belfast, Northern Ireland*
e-mail: fgomez@efn.uncor.edu

ABSTRACT: The La Laja Formation (Early to Middle Cambrian) is one of the oldest units exposed at the base of the lower Paleozoic carbonate platform of the Argentina Precordillera. This is a key unit regarding the hypothesis of the Precordillera as a Laurentia-derived allochthonous terrane currently located in the south-central Andes. According to the faunal affinity and stratigraphic development of the thick Cambrian carbonate bank, the Argentine Precordillera would have been attached to Laurentia. The La Laja Formation contrasts with the rest of the overlying units of the Cambro-Ordovician carbonate platform by being partly mixed carbonates–siliciclastics. This dominantly shallow subtidal unit is internally arranged into several Grand Cycles indicating a complex environmental mosaic, probably with local depocenters related to variable subsidence. This unit records the stabilization of the rifted margin of the Precordillera terrane, prior to the broadening of the carbonate sedimentation during the passive-margin drifting stage.

A high-resolution $\delta^{13}C$ and $\delta^{18}O$ isotope study, in concert with a detailed paleoenvironmental analysis, was carried out to better understand both environmental and chronostratigraphic evolution of the La Laja Formation. Three $\delta^{13}C$ positive excursions were recorded; the first one at the *Glossopleura* biozone within the Soldano Member, the second beginning at the base of the Rivadavia Member, and the third during deposition of the Las Torres Member. Comparisons with other Middle Cambrian curves, in the Precordillera and elsewhere (Rocky Mountains and Great Basin, U.S.A., the western Hunan Province in south China, and the Amadeus, Georgina, and Daly basins in Australia) suggest a global control on these excursions. Mechanisms to produce these positive excursions could be related to high bio-productivity and increased burial of C_{org} (organic carbon) produced by high nutrient influx to the ocean associated with a relative sea-level fall. Local environmental controls could have in part altered the original isotopic signal.

INTRODUCTION

The isotopic signature of diagenetically unaltered marine carbonates can be taken as representative of the fluid (seawater) where the carbonate precipitated. The $\delta^{13}C$ isotopic excursions recorded in marine carbonates result from the combination of global changes in fluxes between different carbon reservoirs of the ocean–atmosphere system, e.g., changes in organic productivity, organic-carbon burial and biological pumping, variations of sedimentation rates and associated accumulation of organic matter, changes in ocean oxygenation state controlling the preservation of organic matter, etc. (Kump 1991; Glumac and Walker 1998; Kump and Arthur 1999; among others). Due to this global control and the presence of secular changes in carbon cycling, chemostratigraphic studies of carbonates have proven to be an invaluable tool where poor biostratigraphic control prevents detailed correlation (Kaufman and Knoll 1995; Pelechaty et al. 1996; Cozzi et al. 2004; among others). In spite of this, regional and/or local controls related to basin evolution, e.g., evaporation, freshwater influx, upwelling water, restriction, aging, and mixing of water masses, etc. (Patterson and Walter 1994; Glumac and Walker 1998; Holmden et al. 1998; Panchuk et al. 2005; Panchuk et al. 2006), and/or possible diagenetic alteration (Banner and Hanson 1990) can modify the primary isotopic signature, and this possibility must be considered when using a chemostratigraphic approach for correlation purposes.

The Argentine Precordillera in the foothills of the Central Andes is well known for its unusual development of Cambrian and lower Ordovician Laurentian-like passive-margin carbonates. Although various regional studies have shed light on the geological evolution of this allochthonous terrane in South America (Ramos et al. 1986; Astini et al. 1995), little detailed sedimentological work has been published and is not readily accessible in the international literature. In the light of poor biostratigraphic control, few reviews and synthesis papers (Astini et al. 1995; Astini 1998; Cañas 1995, 1999; Keller et al. 1998; Keller 1999) have shown the need for enhancing correlation by means of modern high-resolution methods as provided by carbon and oxygen isotope stratigraphy. Although this type of analysis has been applied with success to the Precordillera carbonate record (Buggisch et al. 2003), the interval considered in this paper has not been studied previously.

During the early Paleozoic, shallow epicontinental (or epeiric) seas covered vast areas of the continental interior of Laurentia (Pratt and James 1986). According to its faunal affinity (Benedetto 2004 and references therein) and sedimentary development, the Cambrian carbonate platform of the Argentine Precordillera would have been developed

 1527-1404/07/077-826/$03.00

close to Laurentia. Epeiric platforms are huge flooded areas (from thousand to millions of square kilometers) characterized by flat tops, or very low-gradient profiles (*epeiric ramps*) with very shallow marine waters. Although seawater circulation is not necessarily restricted in these settings (Wright and Burchette 1996), the extension and shallow depth of epeiric seas would have reduced wave energy and tidal influence, inhibiting the thorough mixing and fluent connection between platform-interior and open-sea waters, enhancing salinity and/or temperature stratification in the water column (Allison and Wright 2005; Wells et al. 2005). The poor mixing of waters would also produce geochemical and isotopic gradients between platform interior and more open waters (Holmden et al. 1998; Lukasik et al. 2000; Panchuk et al. 2005; Panchuk et al. 2006). Due to this, care must be taken with the interpretation that the geochemical record of particular Cambrian–Ordovician carbonates is representative of global ocean chemistry, and possible paleoenvironmental and/or diagenetic influences need to be addressed.

Sial et al. (2001) and Sial et al. (2003) made preliminary isotopic studies of the La Laja Formation, although the sampling interval (35 samples through 700 m of section) prevents precise correlations with other curves. Buggisch et al. (2003) published a more detailed $\delta^{13}C$ curve for the whole carbonate platform that allows more precise correlations. In spite of this, because this curve was focused mainly on Upper Cambrian and overlying deposits, most of the Middle Cambrian rocks were not included in the analysis and correlation with other Middle Cambrian curves were not made. Galindo et al. (2004) and Naipauer et al. (2005) also published isolated isotopic data from marbles in the basement cropping out to the east of the Precordillera (Fig. 1A) that may represent equivalents of the lower Paleozoic units in Precordillera.

The purpose of this work is to show high-resolution $\delta^{13}C$ and $\delta^{18}O$ isotope data, in concert with a detailed paleoenvironmental analysis, to the Lower–Middle Cambrian La Laja Formation carbonates. These carbonates crop out at the base of the Argentine Precordillera carbonate bank and are taken to record the progressive stabilization of the rifted margin of the Precordillera terrane, prior to the inception of the broadening carbonate sedimentation during the passive-margin drifting stage of the Precordillera. Furthermore, this study discusses ideas regarding secular oceanic carbon and oxygen isotope fluctuations and local environmental influences.

GEOLOGICAL SETTING

The Argentine Precordillera is a thin-skinned fold and thrust belt located along the forefront of the high Andes between 28° and 33° S (Fig. 1A). Astini (1992) presented a major two fold separation in *western* and *eastern tectofacies* (Fig. 1A) which is useful in understanding the early Paleozoic rock distribution and stratigraphic evolution of the Precordillera. Cambrian–Ordovician passive-margin carbonates and overlying black shales and clastic facies represent the eastern tectofacies cropping out in the Eastern and Central Precordillera (Fig. 1A). A thick clastic wedge of Late Ordovician age including mafic rocks represents the western tectofacies and crops out in the Western Precordillera.

The stratigraphy of the Argentine Precordillera has unique characteristics and differs from that cropping out in neighboring areas of the Central Andes in that it contains a superbly exposed lower Paleozoic carbonate bank at its base that contrasts with the high-latitude clastic domains in Gondwana (Scotese et al. 1999). This has been the reason for considering the Precordillera an allochthonous element in South America (Ramos et al. 1986; Astini et al. 1995). Because stratigraphic and faunal affinities have shown maximum similarities with successions surrounding Laurentia, it was suggested that the Precordillera is a Laurentia derived fragment (Thomas and Astini 1996). This hypothesis has now reached a generalized acceptance after confirmations provided by additional stratigraphy, biostratigraphy (Astini et al. 1995; Benedetto 2004), paleomagnetic data (Rapalini and Astini 1998), basement isotopic signature (Kay et al. 1996), and zircon geochronology (Casquet et al. 2001; Thomas et al. 2004).

The Precordillera exhibits a unique carbonate bank representing a thick (2500 m) largely shallow-water carbonate succession deposited between the Early Cambrian and the Early Ordovician. The Precordillera stratigraphy (Fig. 2) involves a red-bed evaporite-rich basal unit (Cerro Totora Formation) of late Early Cambrian age as shown by *Olenellid* trilobites that represents the rifting stage from Laurentia. The overlying carbonate bank is composed of a Lower to Middle Cambrian mixed carbonate–siliciclastic interval, the La Laja Formation, which is the focus of this study. This mostly shallow subtidal unit is internally arranged in several distinct Grand Cycles (cf. Aitken 1978), indicating a complex environmental mosaic probably with local depocenters related to variable subsidence along an increasingly more stable margin (see Gomez and Astini 2006 for comments regarding Grand Cycles in the La Laja Formation). A stratigraphic gap between Lower and Middle Cambrian deposits and coincidental with the Appalachian Hawke Bay event has more recently been suggested within this unit (Bordonaro 1999; Keller 1999). The thick Los Hornos dolomites (see Fig. 2) cropping out in the northern Precordillera are supposed to be equivalents to the La Laja and Zonda formations. Contrasting facies associations are shown by the overlying Upper Cambrian Zonda and La Flecha formations which are associated with flat-topped platform geometry. In turn, a sharp, low-relief karstic surface representing a basin-wide unconformity separates these dolomites from the overlying Lower Ordovician limestones (La Silla Formation) which were deposited in a detached restricted carbonate platform rimmed by calcarenitic shoals (Cañas 1999). An open-shelf environment, triggered by a third-order sea-level fluctuation, developed during the early Arenig and is represented by the overlying massive, thick-bedded fossil-rich limestones (San Juan Formation).

The Upper Cambrian to Lower Ordovician passive-margin units represent the drifting stage of Precordillera throughout the Iapetus ocean (Astini and Thomas 1999; Thomas and Astini 1999). The approach to Gondwana and the transition into a peripheral foreland stage is indicated by a sudden deepening recorded by the diachronous development of deep-ramp mudstones and black shales during the late Early to early Middle Ordovician (Thomas and Astini 1996, 2003). Abundant K-bentonites through the uppermost carbonate section and the overlying black shales (uppermost San Juan and Gualcamayo formations) indicate approach to an active volcanic-arc setting (Huff et al. 1998). A Middle–Upper Ordovician clastic wedge (Trapiche Group and equivalents) represents a peripheral-foreland-basin response to tectonic loading during Precordillera terrane accretion.

LA LAJA FORMATION STRATIGRAPHY AND BIOSTRATIGRAPHY

The La Laja Formation (late Early to Middle Cambrian) is at the base of the thick Cambro-Ordovician carbonate succession of the Precordillera (Fig. 2). This, and the overlying units of the Cambrian–Ordovician carbonate platform, crop out through the eastern domain in the Villicum and Zonda ranges (Fig. 1A). Isolated blocks of equivalent units (Early to Middle Cambrian in age) also crop out as olistoliths within Ordovician units in the western domain.

The outstanding feature of the La Laja Formation (Borrello 1962) is the arrangement in large-scale alternations of pure and mixed carbonates (carbonates and siliciclastics) that resembles the pattern referred to as *Grand Cycles* (Aitken 1978; Chow and James 1987; James et al. 1989) in early Paleozoic Laurentian stratigraphy. Due to contrasting lithofacies assemblages the La Laja Formation has been divided into five members (Fig. 3): El Estero, Soldano, Rivadavia, Juan Pobre, and Las Torres (Bordonaro 1980; Baldis and Bordonaro 1981, 1984; and Gomez and Astini 2006) that largely record shallow-marine environments with some

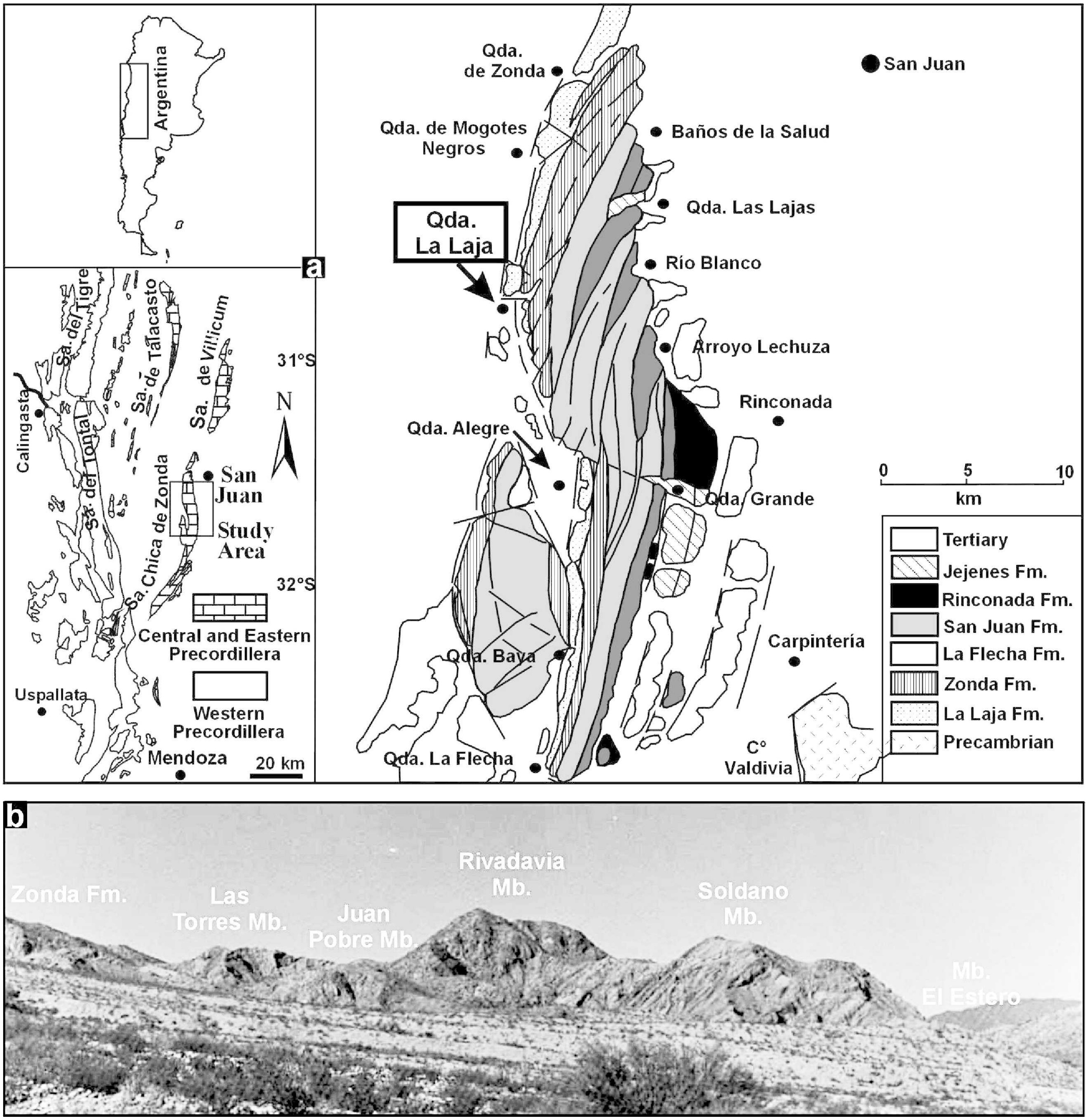

FIG. 1.—**A)** Geologic map of the northern part of the Sierra Chica de Zonda (from Baldis and Bordonaro 1984) and its location within the Eastern Precordillera. **B)** Panoramic view of the La Laja section on the western slope of the Sierra Chica de Zonda. See location in Part A.

evidence of subaerial exposure. Deeper basinal or slope facies are not present in the unit. The present work was carried out in the Quebrada La Laja (31° 33′ 36.5″ S, 68° 44′ 10.3″ W), western margin of the Sierra Chica de Zonda (Eastern Precordillera) (Fig. 1A, B), 13 km to the south of the well-known Zonda Gorge, where the stratotype was defined (Bordonaro 1980; Baldis and Bordonaro 1981).

Borrello (1971) determined a Cambrian age for the La Laja Formation and pointed out strong similarities between the Precordillera and Laurentia trilobites (see also McKerrow et al. 1992 and Vaccari 1994). Borrello (1971) and Bordonaro (2003a, 2003b, and references therein) recognized the *Bonnia–Olenellus* biozone in the lowermost El Estero Member. This biozone has also been recognized in the northern Precordillera (Cerro Totora Formation; Fig. 2) immediately overlying evaporites and red beds (Astini and Vaccari 1996). Keller (1999) and Bordonaro (1999) have suggested the presence of a hiatus between the El Estero and Soldano Members comprising most of the Middle Cambrian biozones (*Plagiura–Poliella*, *Albertella*, and possibly *Glossopleura*). These authors equated this gap with that known throughout the Appalachians

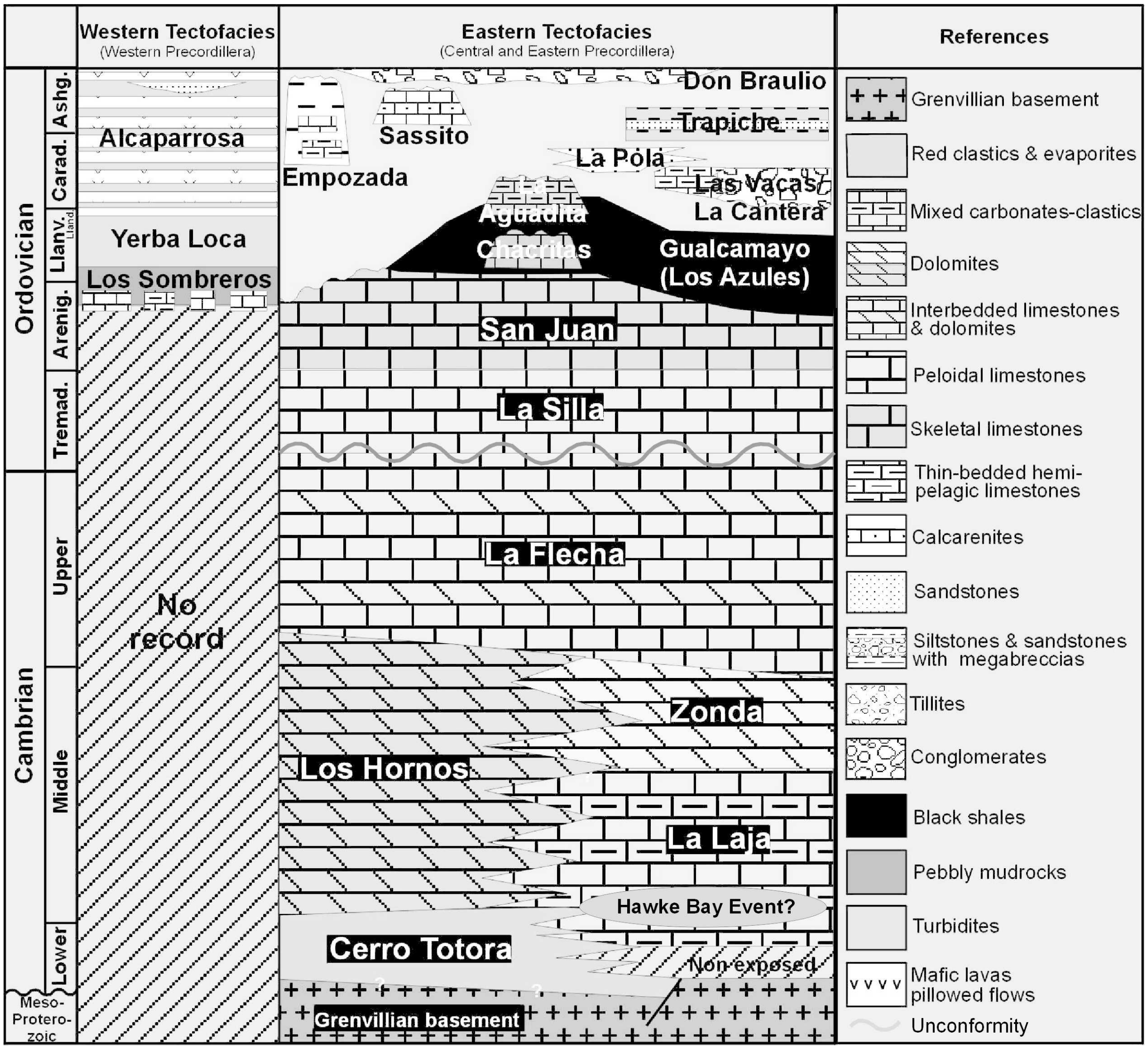

FIG. 2.—Synthetic chronostratigraphic chart of the Cambrian–Ordovician across the Argentine Precordillera (modified from Astini 1998).

as the *Hawke Bay* regressive event (cf. Palmer and James 1979), which separates the Sauk I and Sauk II sequences (cf. Sloss 1963). The *Glossopleura* biozone has been recognized in Cambrian allochthonous units (olistoliths) in Ordovician deposits cropping out to the west (Bordonaro et al. 1993; Bordonaro and Banchig 1996). The Soldano Member has been assigned to the *Glossopleura* (Keller 1999) and *Ehmaniella* (Bordonaro 2003a, 2003b) biozone, whereas the upper part of the La Laja Formation lies in the *Bolaspidella* biozone (BorDonaro 2003a, 2003b). Foglia and Vaccari (2006) have recently recognized the *Glossopleura* biozone in the lower third of the Soldano Member in the La Laja section. Although there is no fossil record in the overlying Zonda Formation, the boundary between the La Laja and the overlying Zonda Formation has been placed coincident with the *Bolaspidella–Cedaria* boundary (Keller et al. 1994). However, as pointed out by Gomez and Astini (2006), this boundary represents a complete rearrangement of the depositional system and hence may involve a possible hiatus.

Conclusive data regarding the precise boundary between biozones, the extent of each biozone, and the presence of a biostratigraphic hiatus have not been yet published, and a revision of the biostratigraphy of the La Laja Formation is necessary in order to improve the chrono-biostratigraphic framework. Most of the available trilobite data belongs to the La Laja Formation at Cerro Molles (southwestern Sierra de Villicum, Fig. 1A), a section that is strongly deformed, and from the Zonda Gorge (northern Sierra Chica de Zonda). There is no detailed biostratigraphic control in the section of the Quebrada La Laja (Fig. 1B) where our sedimentologic analyses and isotopic sampling was carried out. For this reason, our interpretation and correlation is strongly based on a chemostratigraphic approach, and an improvement in the biostratographic framework will be necessary in the future to check or adjust our findings and correlations.

Because the detachment level of various thrusts is commonly within the lower shaly interval of the Cambrian deposits, along the Zonda Range (Fig. 1A) most sections show an incomplete thickness of the La Laja Formation. The more continuous, complete, and undeformed section is exposed 13 km south of the classic site at Zonda Gorge. This is known as the Quebrada La Laja (Fig. 1B). In this section, the upper 15 m of the El Estero Member is followed by the Soldano, Rivadavia, Juan Pobre, and Las Torres Members (Fig. 3) totaling ~ 470 m (Gomez and Astini 2006). The Zonda Formation overlies these deposits.

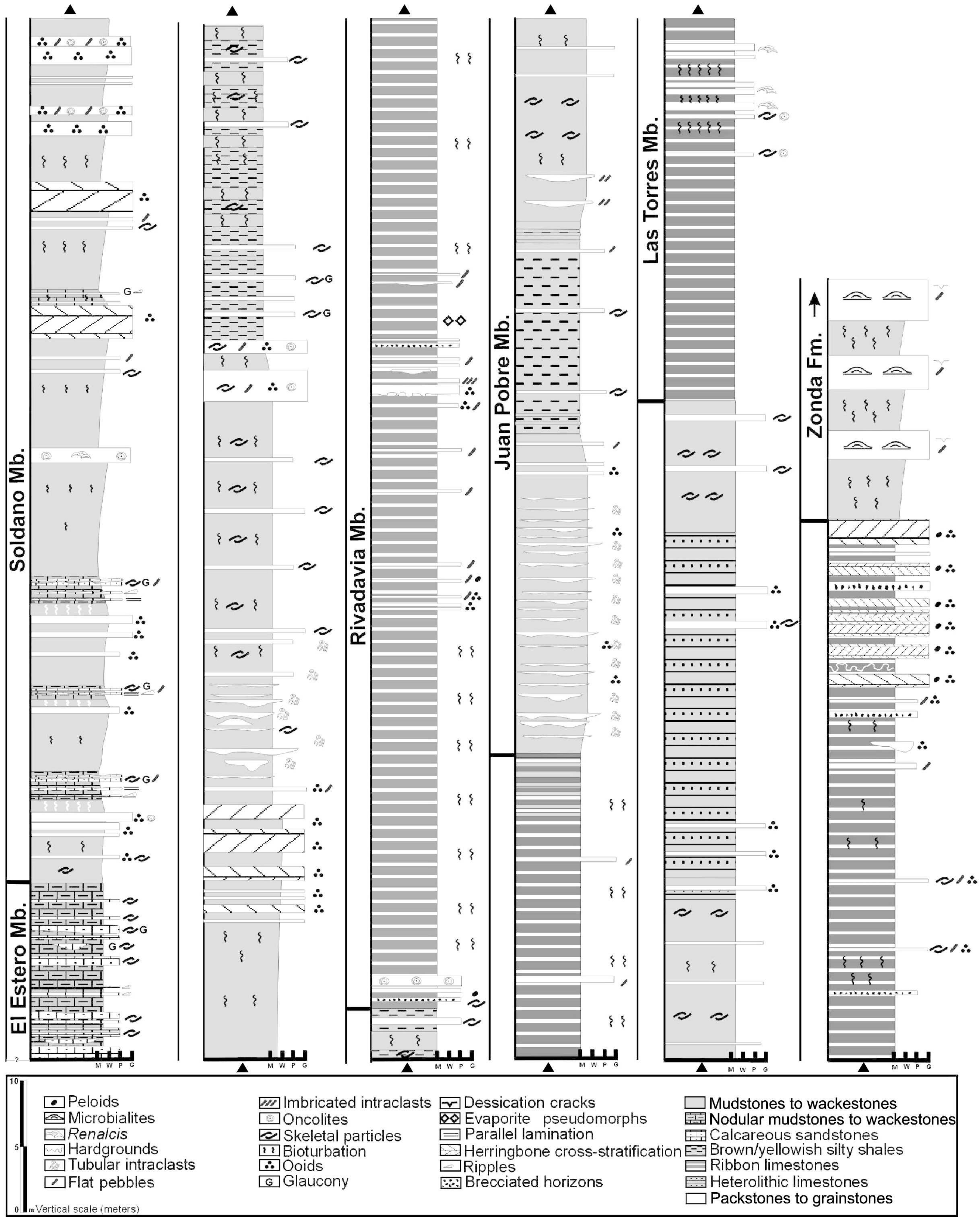

FIG. 3.—Detailed complete stratigraphic log of the La Laja Formation, at the La Laja reference section. The black triangles on top of each column indicate that the section continues.

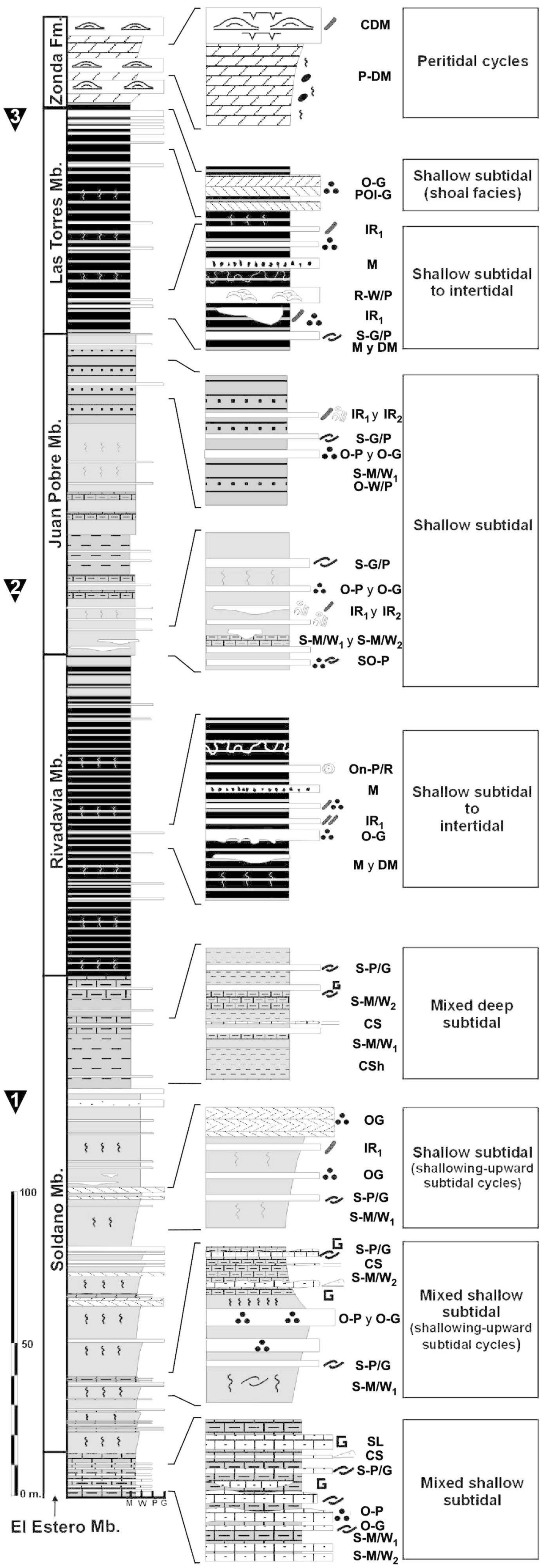

Medium to coarse, calcareous, feldspar-rich sandstones and sandy limestones characterize the El Estero Member. The base of the Soldano Member shows a remarkable cyclicity with capping oolitic shoals at the top of each cycle. This member and the upper Juan Pobre Member contain deeper subtidal intervals, below a storm-weather wave base, with high percentages of fine terrigenous material represented by shaly marls and nodular limestones (Fig. 3). Skeletal-rich and oolite-rich storm beds are recorded in them. Relative shallowing to very shallow subtidal to intertidal environments are recorded in the intermediate Rivadavia Member, with the development of ribbon limestones, intraclastic rudstones, microkarstic surfaces, and exposure breccias (Fig. 3). Distinct herringbone cross-bedded oolite shoals are common at the top of the uppermost Las Torres Member (Keller 1999; Gomez and Astini 2006). The overlying Zonda Formation is represented by development of meter-scale microbial-rich peritidal cycles (Gomez and Astini 2006).

METHODOLOGY

A detailed stratigraphic analysis (Fig. 3) was carried out from outcrops of the La Laja section, and hand samples were collected at roughly 1–3 m intervals for petrography and geochemistry. Thin sections and polished slabs of representative samples of field lithofacies were made and screened under petrographic microscopy in order to determine component microfacies and to aid in paleoenvironmental analysis. On the basis of the petrography, we find that the primary fabrics of the rock are generally well preserved although some degree of recrystalization is present in a few samples. Two hundred samples consisting predominantly of micritic limestones (mudstones, wackestones, and packstones) were selected for isotopic analysis. A few samples of calcarenitic limestones (grainstones) and microbial dolostones were also analyzed (see Tables A and B in JSR's Data Archive, URL in Acknowledgments section).

Between 0.4 and 0.9 mg of each sample were placed in 6 ml glass vials and inserted into a holder maintained at 50°C. After temperature equilibration had been achieved (2.5 hours) each sample was automatically flushed with helium and a few drops of 100%+ orthophosphoric acid deposited onto the samples. To ensure complete reaction the samples were left overnight. The next day the samples were taken to the mass spectrometer and left for a further 2.5 hours to ensure room-temperature equilibration. Every sample was repeated and an in-house standard, calibrated against the IAEA Standard NBS19 (V-PDB, Vienna Pee Dee Belemnite), was analyzed every 4 or 5 samples. Analytical precision for both carbon and oxygen was found to be better than 0.2 per mil.

PALEOENVIRONMENTS OF THE LA LAJA FORMATION

Detailed stratigraphy, main lithofacies, and sedimentologic features of the La Laja Formation are shown in Figure 3 and discussed in Gomez and Astini (2005, 2006). A brief description follows of the main features of the field lithofacies; constituent microfacies are summarized in Table I. Paleoenvironmental interpretations are shown in the stratigraphic logs of Figure 4.

Mixed Deep Subtidal

This lithofacies association is commonly seen in the Soldano and Juan Pobre members (Figs. 3, 4) and characterized by intervals containing abundant fine siliciclastic material, hence elsewhere described as

←

FIG. 4.—Simplified stratigraphic column of the La Laja Formation showing the main lithofacies and details of distinct lithofacies associations. See Table 1 and text for further details. The black triangles indicate the top of each Grand Cycle as proposed in Gomez and Astini (2006).

marlstones. It is represented by thoroughly bioturbated, glauconite-bearing brownish to yellowish calcareous siltstones and silty shales and thin-bedded nodular mudstones to wackestones (microfacies CSh, CS, S-M/W_1, and S-M/W_2, Table 1). Thin tabular beds of graded skeletal packstones to grainstones (microfacies S-P/G), with erosional bases and without evidence of wave reworking and/or amalgamation, are interpreted as interbedded distal storm layers. This lithofacies association indicates deposition below storm wave base, with abundant influx of fine siliciclastic material (Gomez and Astini 2006). Thin laminated glauconite-rich layers indicate low sedimentation rates and condensation (cf. Odin and Matter 1981).

Mixed Shallow Subtidal

This lithofacies association is recorded at the top of the El Estero Member (Figs. 3, 4, Table 1) and is represented by coarse (quartz- and feldspar-rich) sandy limestones, calcareous sandstones (microfacies SL) and brownish to greenish calcareous siltstones (microfacies CS) within thin-bedded to nodular bioturbated skeletal mudstones to wackestones (microfacies S-M/W_1 and S-M/W_2). Skeletal and oolitic packstones and grainstones are also common (microfacies S-P/G, O-P, and O-G). The calcarenites are graded, wave-reworked, lenticular to wavy, and where in more continuous beds, occasionally amalgamated (thickness up to 30 cm) with erosional bases. This association represents shallow subtidal environments above storm wave base with sporadic influx of nearshore siliciclastic material (derived from cratonic areas) transported into carbonate-dominated environments by storm surges (*punctuated mixing*, cf. Mount 1984). Tabular calcarenites represent storm deposits.

Toward the transition between the El Estero and Soldano members, relatively "pure" carbonates (devoid of siliciclastics) cyclically alternate with siliciclastics-bearing carbonates. These deposits are arranged into meter-scale (up to 10 m) shallowing-upward shallow subtidal cycles (Figs. 3, 4, Table 1) that start with thin-bedded to nodular bioturbated mudstones to skeletal wackestones (microfacies S-M/W_1) interbedded with skeletal, oolitic, and intraclastic packstones to grainstones (microfacies S-P/G, O-P, O-G, and IR_1). Calcarenite beds of brownish to yellowish skeletal and oolitic, siliciclastics- and glauconite-bearing packstones to grainstones (microfacies S-P/G and O-P), interbedded in bioturbated mudstones and skeletal wackestones (microfacies S-M/W_2), overlie these lithofacies. Thin tabular to lenticular beds of siltstones with angular to subangular quartz grains (microfacies CS) are also common and indicate the influx of siliciclastic material from nearshore areas. These cycles represent a low-energy shallow subtidal environment, occasionally affected by storms. During shallowing, terrigenous influx prograded into the basin and was transported into a subtidal environment (Gomez and Astini 2006). Evidence of wave reworking atop these cycles indicates relatively shallow depths and deposition above fair-weather wave base.

Shallow Subtidal

These facies associations include both cyclically arranged and noncyclic shallow subtidal deposits devoid of significant siliciclastic material (see Figs. 3 and 4).

Shallowing-upward subtidal cycles (5–15 m) are recorded in the mid-Soldano Member and are represented by bioturbated skeletal mudstones to wackestones (microfacies S-M/W_1) interbedded with thin-bedded skeletal, intraclastic, and oolitic packstones to grainstones (microfacies S-P/G, IR_1 and O-G). Cross-bedded oolític grainstone caps of up to 1 m (microfacies O-G) overlie these deposits and represent high-energy oolitic shoals prograding onto deeper subtidal deposits with a decrease in accommodation space. The presence of herringbone cross-stratification indicates a tidal influence. The absence of siliciclastic material indicates that these calcarenitic shoals were developed sheltered or far enough from terrigenous influx to avoid mixing even during storms. No evidence of subaerial exposure was found on the tops of these cycles, indicating that the sediment redistribution processes (by waves and tides) avoided aggradation and protracted exposure (Gomez and Astini 2006). Similar cycles are described elsewhere and interpreted as subtidal aggradation cycles (e.g., Aigner 1985; Osleger 1991; Osleger and Read 1991; Srinivasan and Walker 1993; among others).

Shallow subtidal deposits are commonly seen in the Soldano and Juan Pobre members and are represented by bioturbated mudstones to skeletal wackestones (microfacies S-M/W_1 and S-M/W_2) punctuated by largely tabular (up to 20 cm) skeletal, skeletal–oolitic, and oolitic packstones to grainstones (microfacies S-P/G, O-P, SO-P, and P-G/P) and intraclastic rudstones (IR_1 and IR_2). The packstones, rudstones, and grainstones are tabular to lenticular beds. Coarser-grained beds show sharp bases, and occasional gutter and casts, and are internally graded, representing storm deposits. Some storm beds include flat pebbles and intraclasts with complex tube-like shapes (tubular intraclasts, microfacies IR_2), interpreted as early-cemented trace fossils exhumed and reworked during storms (Gomez and Astini 2004, 2006). Gutters and casts are commonly interpreted as produced by turbulent helical flows during storms in shallow subtidal environments (Kreisa 1981; Aigner 1985; Myrow 1992, 1994). Alternatively, they have been interpreted as a product of supratidal or intertidal exposure and runoff (Bridges 1972; Duringer and Vecsei 1998) although no evidence, such as meteoric diagenesis or pedogenic features, were found to support this hypothesis (Gomez and Astini 2006). This association represents shallow subtidal deposits punctuated by episodic storms.

Laminated and thin bedded heterolithic facies represented by bioturbated mudstones to skeletal wackestones (microfacies S-M/W_1), alternating with oolitic wackestones and packstones (microfacies O-W/P) are common deposits in the uppermost part of the Juan Pobre Member. Tabular beds of skeletal and oolitic packstones to grainstones (microfacies S-P/G, O-P, and O-G) and intraclastic packstones to rudstones (microfacies IR_1 and IR_2) are also present. These lithofacies represents a low-energy setting (restricted lagoon), where deposition of lime mud predominated at the lee sides of oolitic shoals (back-shoal setting). In this environment waves and storms would have transported ooids across the lagoon. More tabular ooid-rich beds represent event deposits produced by storms. Similar back-shoal deposits with oolitic shoals sheltering low-energy lagoon environments are present to the northwest of Andros Island (Bahamas) (see Ball 1967; among others) and have been interpreted elsewhere in the stratigraphic record.

Shallow Subtidal to Intertidal

Ribbon limestones (cf. Demicco 1983) represented by slightly to moderately bioturbated dark gray to black mudstones and laminated yellowish dolomudstones (microfacies M and DM) interbedded with tabular to lenticular beds of skeletal, oolitic, peloidal, and oncolitic packstones and grainstones (microfacies S-P/G, O-G, POI-G, and On-P/R) and intraclastic rudstones (microfacies IR_1) dominate in the Rivadavia and Las Torres members and represent shallow subtidal to intertidal environments (Gomez and Astini 2006). In the Rivadavia Member, the presence of large *Girvanella*-bearing oncolites (~ 1–2 cm diameter) and aggregates indicate a low-energy, very shallow and well-illuminated environment (cf. Flügel 1982, 2004; Peryt 1983; Tucker and Wright 1990). Oolitic grainstones (microfacies O-G), breccias and pseudobreccias (cf. Demicco and Hardie 1994) are also present. Brecciated horizons, microkarstic features, and hardground surfaces indicate frequent subaerial exposure, and local development of evaporite pseudomorphs indicates environmental restriction under an arid climate. Altogether these features point to dominantly intertidal environments with frequent subaerial exposure (e.g., Demicco and Hardie 1994). Some discrete

TABLE 1.—*Lithofacies, bedding characteristics, and main constituent microfacies of the La Laja Formation, Cambrian of the Argentine Precordillera.*

Lithofacies	Bedding and thickness	Contacts	Color	Microfacies constituents
Thin-bedded and nodular limestones	Tabular beds 2–10 cm thick (occasionally separated by shaly partings) sometimes developing a stylonodular pattern.	Sharp boundaries represented by stylolitic joints and dissolution seams where insoluble residue and dolomite are concentrated.	Light to medium gray. Trace fossils are yellowish due to selective dolomitization. Brownish to yellowish shaly partings and red ferruginous crusts are also present.	**S-M/W$_1$**-Mudstones to skeletal wackestones.. **S-M/W$_2$**-Largely nodular mudstones to skeletal wackestones with variable amount of siliciclastic
Heterolithic limestones	Irregular bedding of occasionally bioclastic mudstones and skeletal wackestones (up to 1–2 cm) alternating with oolitic packstones (between 2–3 cm and 1–2 mm).	Relatively sharp contacts locally disrupted by bioturbation and enhanced by pressure solution.	Light gray. Dissolution seems are brownish to yellowish.	**S-M/W$_1$**-Mudstones to skeletal wackestones **O-W/P**-Oolitic wackestones to packstones
Ribbon limestones	Rhythmic bedding (1–5 cm) of occasionally peloidal mudstones alternating with laminated silty dolomudstones. Mottled fabric where pervasive bioturbation is present.	Sharp boundaries associated with hardgrounds and microkarstic surfaces and diffuse boundaries where little substrate consistence (softground). Contacts commonly affected by pressure solution.	Dark gray mudstones alternating with yellowish dolomudstones. Bioturbation (yellowish) diagenetically enhanced by selective dolomitization.	**M**-Mudstones **DM**-Dolomudstones to dolosiltstones
Muddy limestones with *Renalcis* aggregates	Laterally continuous massive beds up to 3 m thick. Internally alternating bioturbated mudstones (1–5 cm) and packstones (3–4 cm) with *Renalcis* aggregates (3–5 mm diameter). Pseudostratification is apparent due to stylolitic joints.	Interbedded with thin-bedded to nodular limestones. Sharp contacts.	Alternating light to medium gray mudstones with darker *Renalcis*-bearing packstones. The *Renalcis* aggregates look like dark gray oncoids.	**R-W/P**-Wackestones to packstones with *Renalcis* aggregates.
Calcarenitic limestones	Tabular to lenticular beds of variable thickness (up to 20 cm). Normally graded and occasionally amalgamated beds within thin-bedded to nodular limestones.	Beds display sharp (erosional) lower contacts, occasionally developed on hardgrounds.	Light to medium gray. Often brownish to yellowish due to the oxidation of iron-rich minerals (glauconite) or the presence of siliciclastic material.	**S-P/G**-Skeletal Packstones to grainstones. **O-P**-Oolitic packstones. **SO-P**-Skeletal–oolitic packstones. **P-P/G**-Polymictic grainstones to packstones. **O-G**-Oolitic grainstones. **POI-G**-Peloidal–oolitic—intraclastic grainstones.
Intraclastic rudstones	Tabular to lenticular occasionally graded and seldom amalgamated beds. Thickness up to 20 cm.	Erosional lower contacts occasionally developed on hardgrounds or microkarstic surfaces. Also filling gutters and casts within thin-bedded to nodular limestones.	From light/medium (tubular intraclasts- L_2) to dark gray /black (flat pebbles-L_1).	**IR$_1$**-Intraclastic rudstones (flat pebbles). **IR$_2$**-Intraclastic rudstones (exhumed tubular intraclasts).
Oncolitic limestones	Tabular beds up to 40–50 cm thick. Oncolites up to 2–3 cm in diameter.	Sharp lower contacts interbedded within ribbon limestones.	Dark gray.	**On-P/R**-*Girvanella*-rich oncolitic rudstones.
Breccias	Tabular to lenticular beds of variable thickness, generally up to 40–50 cm.	Erosional lower contacts associated with hardgrounds and/or microkarstic surfaces.	Dark-gray clasts (mudstones) in a yellowish selectively dolomitized matrix.	**M**-Mudstones
Pseudobreccias	Tabular beds up to 30–40 cm. Highly bioturbated horizons with brecciated appearance.	Irregular and diffuse contacts occasionally enhanced by pressure solution.	Dark gray to black pseudoclasts and yellowish matrix due to selective dolomitization.	**P-M**-Ocasionally peloidal mudstones **DM**-Dolomudstones
Massive dolostones	Pervasively dolomitized massive horizons. Tabular beds up to 2 m thick. Bioturbation is also common.	Sharply overlying cryptomicrobial dolostones.	Medium to dark gray.	**P-DM**-Peloidal dolomudstones.
Cryptomicrobial dolostones.	Internally laminated tabular beds up to 2–3 m thick. Thin planar to wavy laminae with fenestral porosity and desiccation cracks.	Sharp lower contacts occasionally associated with hardgrounds and microkarstic surfaces.	Light gray to whitish.	**CDM**-Cryptomicrobial dolomudstones.
Brownish to yellowish calcareous silty shales.	Internally laminated thin-bedded to nodular. Laminae up to 2–3 mm.	Nodular fabric, contacts affected by pressure solution.	Brownish/greenish to yellowish.	**CSh**-Calcareous silty shales and micaceous muds.
Brownish to greenish calcareous silts.	Lenticular beds up to 3 cm thick. Internal cross lamination and parallel lamination.	Sharply overlying thin-bedded to nodular limestones.	Brownish/greenish to yellowish.	**CS**-Calcareous silts
Sandy limestones and calcareous sandstones	Lenticular beds up to 30 cm. Often amalgamated, internally laminated beds with wave-reworking features.	Erosional bases, sharply overlying thin-bedded to nodular limestones.	Brownish to yellowish. Occasionally greenish due to abundant glauconite.	**SL**-Sandy limestones and calcareous sandstones.

intervals of brecciated horizons (microfacies M) and beds with *Renalcis* aggregates (micorfacies R-W/P) were also recorded in the Las Torres Member (Gomez and Astini 2005). On top of the Las Torres Member, cross-bedded peloidal–oolitic–intraclastic grainstones (microfacies POI-G) were recorded, representing high-energy calcarenitic shoals deposited in a shallow subtidal environment.

Peritidal cycles

Shallowing-upward cycles (up to 4–6 m in thickness) are common at the base of the Zonda Formation. Dark bioturbated and pervasively dolomitized peloidal mudstones to wackestones (microfacies P-DM) were deposited in a shallow subtidal environment and represent the lower hemicycle. Light-colored cryptomicrobial dolostones (microfacies CDM) are the most conspicuous lithofacies of the upper hemicycle. The presence of fenestral porosity, desiccation cracks, microstromatolites, flat-pebble conglomerates, and pervasive dolomitization indicates processes common in intertidal to supratidal arid environments. Cycles like these are commonly described in the literature and referred to peritidal cycles (Hardie 1986; Demicco and Hardie 1994; Tucker and Wright 1990, among others).

STABLE-ISOTOPE ANALYSIS

The complete carbon and oxygen isotopic record is shown in Figure 5, Appendices A and B (see Acknowledgments section for URL of JSR's Data Archive), and the lithofacies and facies associations where the isotopic data was recorded are shown in Figures 3 and 4 and in Table 1.

The $\delta^{13}C$ values fluctuate between −2.3‰ and +1.6‰ and the $\delta^{18}O$ between −10.9‰ and −4.5‰ although 93.85% of the $\delta^{18}O$ values range between −6‰ and −9‰ (relative to the VPDB standard). Whereas $\delta^{18}O$ is more prone to diagenetic alteration and care must be taken when interpreting the data, the $\delta^{13}C$ signal is more difficult to alter. As pointed out by Banner and Hanson (1990) and Gao and Land (1991), the massive resetting of $\delta^{13}C$ primary values during (open-system) meteoric diagenesis requires high water/rock ratios (around 10^3, which are considered to be unrealistic). This indicates that the $\delta^{13}C$ isotopic composition is strongly rock buffered during meteoric diagenesis and the primary signal is prone to be preserved. Because the range of variability shown by the $\delta^{13}C$ (and to a less degree $\delta^{18}O$) isotope record in the La Laja Formation is consistent with Middle Cambrian values and can be correlated with curves recorded by other authors (Srinivasan 1993; Brasier and Shukov 1998; Montañez et al. 2000; Buggisch et al. 2003; Zhu et al. 2004; Saltzman 2005; Lindsay et al. 2005), this is indicative that a primary (diagenetically unaltered) signal is recorded.

Unfortunately, late diagenetic cements in the La Laja Formation could not be analyzed in this study. In spite of this, massive calcite veins recorded in the Upper Cambrian La Flecha Formation (Buggisch et al. 2003) yield much more negative values of $\delta^{18}O$ (between −11 and −18‰) when compared with the La Laja Formation values. This range of more negative isotopic signatures may be related to late diagenetic fluids during late burial, or they are more likely the result of Tertiary Andean deformation.

The lower 50 m of the section shows a highly variable and saw-tooth pattern, with $\delta^{13}C$ values ranging between −0.2 ‰ and −2.3‰. In this interval, the lower 15 m associated with mixed subtidal lithofacies, deposited above the fair-weather wave base, shows the most negative $\delta^{18}O$ values of up to −10.9‰. A sharp change toward less negative $\delta^{18}O$ values was recorded above this interval. Although this 50 m interval has a recurrent $\delta^{13}C$ signal, in the relatively deep-water mudstones of one of the more distinct cycles a positive shift exceeds 1‰ (Soldano Member Positive Excursion, SMPE). This peak seems one of the strongest signals in the curve (Fig. 5).

After the Soldano Member $\delta^{13}C$ positive excursion (55 m from the base), reaching +1.1‰, the curve becomes negative and gradually loses the saw-tooth pattern. Following a stable interval of 25 m, with values close to −1‰, a more negative interval (33 m) is evident, reaching values close −2‰ followed by an abrupt positive excursion of up to +1.6‰ (Rivadavia Member positive excursion, RMPE). An abrupt change toward less negative $\delta^{18}O$ values is also associated with this excursion. After this $\delta^{13}C$ positive interval of 40 m and a mean value of +1.2‰ a gradual change toward negative values reaching −1.6 ‰ is recorded. Values near −1.5‰ are sustained for ~ 100 m, with the exception of a short excursion to −0.3‰. Then, a positive excursion of 25 m shows values up to +0.9‰ (Las Torres Member positive excursion, LTMPE). On top of the Las Torres Member, an abrupt shift toward more negative $\delta^{18}O$ values (close to −8‰) is recorded. Because this apparent shift corresponds to only one sample, a possible diagenetic effect can be suggested. This negative $\delta^{18}O$ shift is followed by an abrupt change toward less negative $\delta^{18}O$ values (up to −4.5‰) recorded at the base of the Zonda Formation.

The excursions are highly asymmetrical, with a sharp positive (or less negative) start and then a gradual shift toward more negative values. This pattern has also been recorded in the other published Middle Cambrian curves (see next section) (Montañez et al. 2000; Buggisch et al. 2003; Zhu et al. 2004; Saltzman 2005; Lindsay et al. 2005).

ISOTOPE RECORD AND PALEOENVIRONMENTAL INFLUENCE

The Cerro Totora (late Early Cambrian, Astini and Vaccari 1996) and La Laja formations (late Early to Middle Cambrian) represent, respectively, the late rifting and early passive margin stages associated with the separation of the Precordillera from Laurentia (Thomas and Astini 1996; Astini 1998). The synrift history is represented by a succession of evaporites, dolostones, and red beds with *olenellid* trilobites at the top indicating a late Early Cambrian age. The Cerro Totora Formation represents mixed tidal-flat deposits developed in an arid climate and is partially equivalent to the mixed shallow subtidal deposits of the El Estero Member (La Laja Formation). As shown by the more radiogenic Sr^{87}/Sr^{86} isotopic record and terrigenous input, the Cerro Totora Formation shows influence of continental runoff and has been interpreted as deposited in fault-bounded basins partially open to marine circulation (Thomas et al. 2001). This continental influence was gradually lost toward the Upper Cambrian, evolving from an attached to a detached flat-topped passive-margin carbonate platform. In this context the siliciclastics-rich La Laja Formation represents the transitional stage.

Because most of the outcrops of the Precordillera carbonate platform are largely along depositional strike and the only evidence of Cambrian outer-shelf or slope facies is recorded as olistoliths in Ordovician strata to the west (Benedetto and Vaccari 1992; Bordonaro and Banchig 1996), the depositional strike and platform profile is not completely clear. No high-energy shoreface deposits were recorded in the La Laja Formation, and, according to facies analyses, episodic storms and tides influenced the distribution of sediments along the platform. The presence of gutter casts and storm layers suggests that episodic strong storm surges affected the platform, as is common in attached epeiric platforms (e.g., Lukasik et al. 2000). As pointed out by Astini et al. (1996), the Precordillera carbonate platform would have had a minimum width of 400 km.

There are no obvious systematic variations of C isotopes in the La Laja Formation with recorded paleoenvironments (Fig. 6). The isotopic values in shallow and deeper subtidal deposits partly overlap with those recorded in shallow subtidal to intertidal facies and also with the isotopic signature of peritidal carbonates. The range of $\delta^{18}O$ values between deeper subtidal and shallow subtidal to intertidal deposits also overlaps (Fig. 6), although the average $\delta^{18}O$ value of shallow subtidal to intertidal is slightly enriched. Of note is that the ^{18}O enrichment recorded within

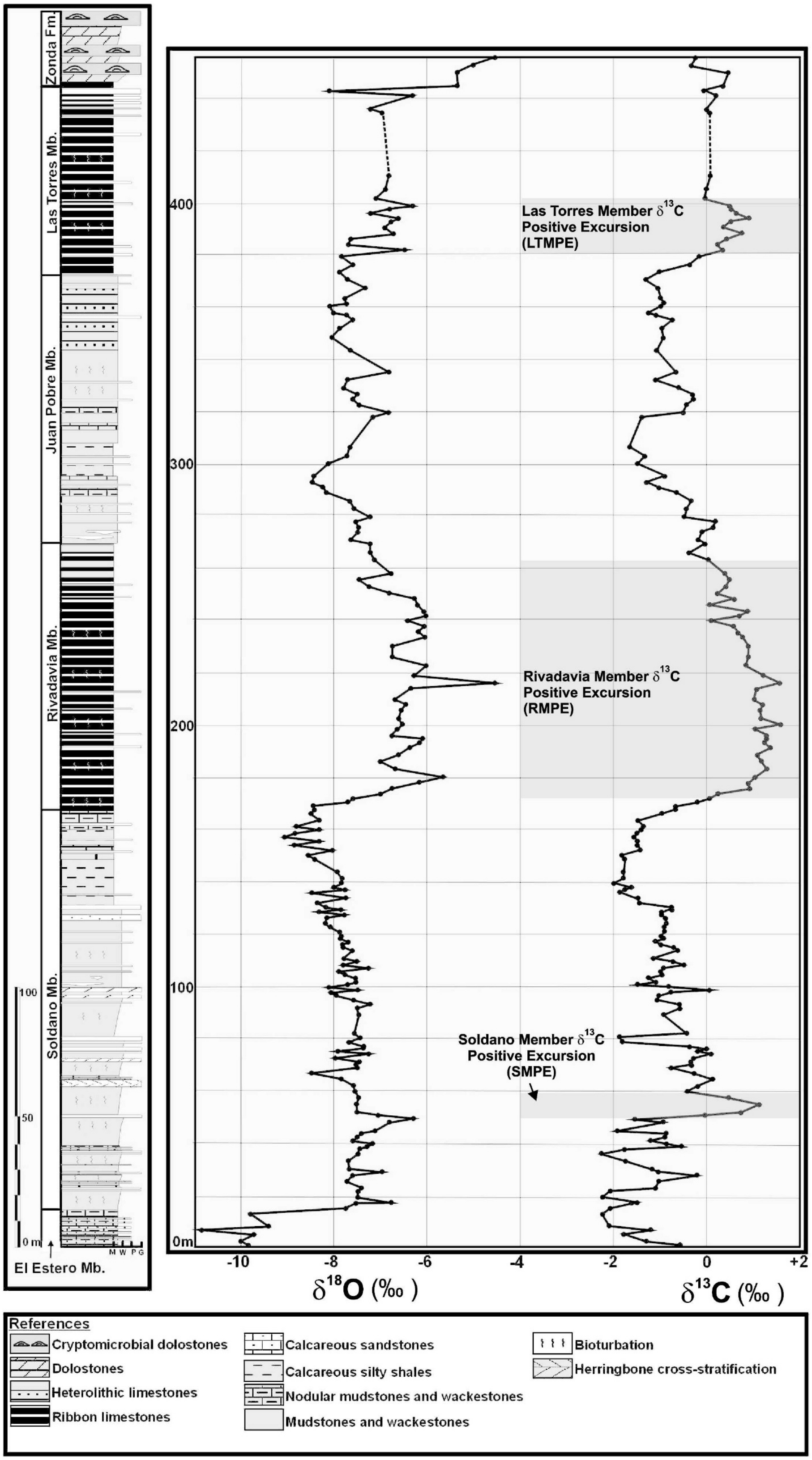

FIG. 5.—Carbon and Oxygen isotope curves through the stratigraphy of the La Laja Formation at the La Laja section. SMPE = Soldano Member Positive Excursion; RMPE = Rivadavia Member Positive Excursion; LTMPE = Las Torres Member Positive Excursion.

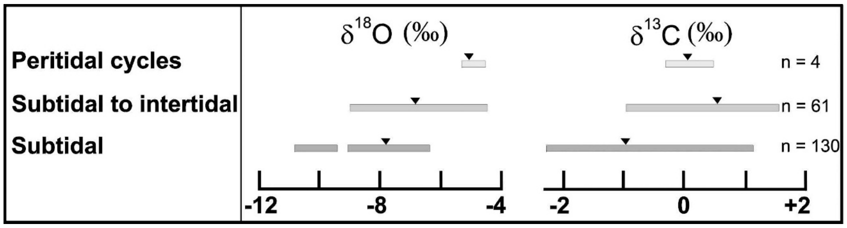

FIG. 6.—Ranges of C and O isotope values for various lithofacies studied. The number of samples (*n*) and mean values (black triangles) are shown. Gap in $\delta^{18}O$ indicates the strong shift observed near the base of the curve (see Fig. 5).

peritidal cycles is probably due to increased evaporation within intertidal to supratidal environments under arid climates.

The highly variable pattern of $\delta^{13}C$ values of the lowermost 100 m of the section could be related to a primary cyclic nature of the stratigraphic interval. Although some degree of diagenetic overprint cannot be ruled out, petrographic evidence of meteoric diagenesis (such as dissolution fabrics, pendant or meniscus cements in calcarenitic lithofacies, etc.) has not been observed in these deposits. In the relatively deep-water mudstones in the lower 50 m of the Soldano Member (*Glossopleura* biozone), a distinct positive shift exceeding 1‰ can be related to either a local signature of sea-level rise that restricted the light carbon riverine sources farther landward or a potentially global signature that may also be recorded in the Daly section in Australia (Lindsay et al. 2005) and also probably in southern China and the Rocky Mountains–Great Basin sections (Zhu et al. 2004; Montañez et al. 2000) (Fig. 7). Shallowing-upward subtidal cycles with variable siliciclastic influx associated with relative sea-level changes developed through the transition between the El Estero and Soldano members (Gomez and Astini 2006). Toward the mid-section of the Soldano Member the terrigenous influx was gradually lost and cycles devoid of siliciclastics developed. These cycles represent high-energy oolitic shoals prograding over more restricted lagoon deposits due to decreasing accommodation space. In this setting, changes in the degree of restriction of the water masses can prevent the mixing and produce salinity and/or temperature stratification (Allison and Wright 2005; Wells et al. 2005). The expansion and contraction of isotopically different water masses (open vs. more restricted) and local-scale carbon cycle processes (e.g., remineralization of organic matter, evaporation, etc.) can be responsible for lateral variations in $\delta^{13}C$ across the basin (cf. Holmden et al. 1998; Panchuk et al. 2005; Panchuk et al. 2006). As pointed out by Patterson and Walter (1994), restricted circulation across the Bahamas and Florida Bay produce ^{13}C-depleted waters by as much as 4‰ compared with open-ocean waters. According to this, during deposition of the Soldano Member, relative sea-level changes could have produced changes in the restriction, triggering the variable isotopic record shown in the $\delta^{13}C$ curve. A long residence time of seawater in restricted areas such as lagoon environments would produce the "aging" of water masses (cf. Patterson and Walter 1994; Holmden et al. 1998; Panchuk et al. 2005), and remineralization of organic matter and/or continental freshwater input could produce ^{13}C-depleted waters in comparison with more open-marine waters. The influence of ^{13}C-depleted waters associated with soil development is not clear during the Cambrian because vascular plants did not appear until the Silurian. In spite of this, increasing evidence indicates that a microbial biosphere had adapted to subaerial conditions and environments as late as the Proterozoic (Horodyski and Knauth 1994; Gutzmer and Beukes 1998; Watanabe et al. 2000; Prave 2002; Dott 2003), although the influence that this non marine biomass may have had on the global (and/or local) carbon cycle is not completely understood. Beeunas and Knauth (1985) proposed that Precambrian ^{13}C-depleted carbonates of the Mescal Limestones (Arizona, U.S.A.) could be associated with some sort of terrestrial vegetative cover (maybe algal in nature) influencing the isotopic signature of carbonates (see also Vahrenkamp and Rossinsky 1987). During the deposition of the La Laja Formation, coastal runoff associated with a vegetative cover of this sort could have produced the input of ^{13}C-depleted water into restricted water masses. Relative sea-level changes would have controlled the degree of restriction and the complex interaction of isotopically different water masses, producing the observed pattern. In order to test this hypothesis, additional isotopic analyses are underway in Cambrian blocks (olistoliths) that record more open-marine conditions (outer-shelf environments).

Due to increasing accommodation space the cyclic stacking of facies and the presence of siliciclastics, as well as the saw-tooth pattern of the $\delta^{13}C$ curve, is gradually lost toward the mid-section of the Soldano Member. This could indicate more open-marine conditions where the influence of terrestrial runoff is diminished as well as the potential for meteoric diagenetic alteration.

The 1‰ negative isotopic excursion of the clastic interval on top of the Soldano Member is followed by the abrupt ~ 2‰ positive shift at the base of the Rivadavia Member (Fig. 5). The siliciclastic interval (brownish to yellowish glauconite-rich calcareous shales and siltstones) records low $\delta^{13}C$ values. Glauconite suggests reducing conditions during early post depositional diagenesis that could have favored organic-matter remineralization (e.g., anaerobic respiration and fermentation) partially responsible for the observed low $\delta^{13}C$ values. The dark gray to black organic-rich mudstones of the Rivadavia Member (Baldis and Bordonaro 1981) represent a low-energy, restricted, very shallow subtidal to intertidal environment (Gomez and Astini 2006). Under such conditions, the restriction of water masses and remineralization of organic matter should produce a depleted $\delta^{13}C$ signal. However, an abrupt positive shift is recorded (Fig. 5). This shift could be associated with increased evaporation in such a restricted and occasionally subaerially exposed setting (this could also explain the more positive $\delta^{18}O$ values). In spite of this, lithofacies remain without significant changes throughout the curve, yet the curve shows an abrupt positive excursion with a steep slope at the beginning followed by a stable interval close to +1.5‰ $\delta^{13}C$ and a gradual decrease (all during the Rivadavia Member), indicating other than local environmental influences.

The abrupt change from deeper mixed subtidal deposits (top of Soldano Member) toward very shallow subtidal to intertidal deposits (Rivadavia Member) could be associated with a relative sea-level fall. Third-order relative sea-level changes have been recorded for various stages in the Middle Cambrian (e.g., *Glossopleura* and *Bathyuriscus Elrathina*/*Ehmaniella* or equivalent biozones, *Ehmaniella–Bolaspidella* and *Bolaspidella–Cedaria*) in various basins around the world including the Rocky Mountains (Aitken 1978 and Aitken 1981), the Great Basin (Palmer 1971b; Sundberg 1991), the Southern Appalachians (Read 1989; Koerschner and Read 1989; Kozar et al. 1990; Srinivasan and Walker 1993; Rankey et al. 1994), Australia (Lindsay et al. 2005) and the North and South China basins (Meng and Tucker 1997; Zhu et al. 2004). Although some of these are poorly constrained due to limited resolution of trilobite biostratigraphy (Fig. 7), they seem to indicate the presence of a eustatic sea-level signal.

Following the Rivadavia Member positive excursion, there is a decrease toward negative values in the siliciclastics-rich Juan Pobre interval (Fig. 5). After a shift toward higher values, a positive peak at the base of the Las Torres Member (*Bolsapidella* biozone) is recorded. This excursion

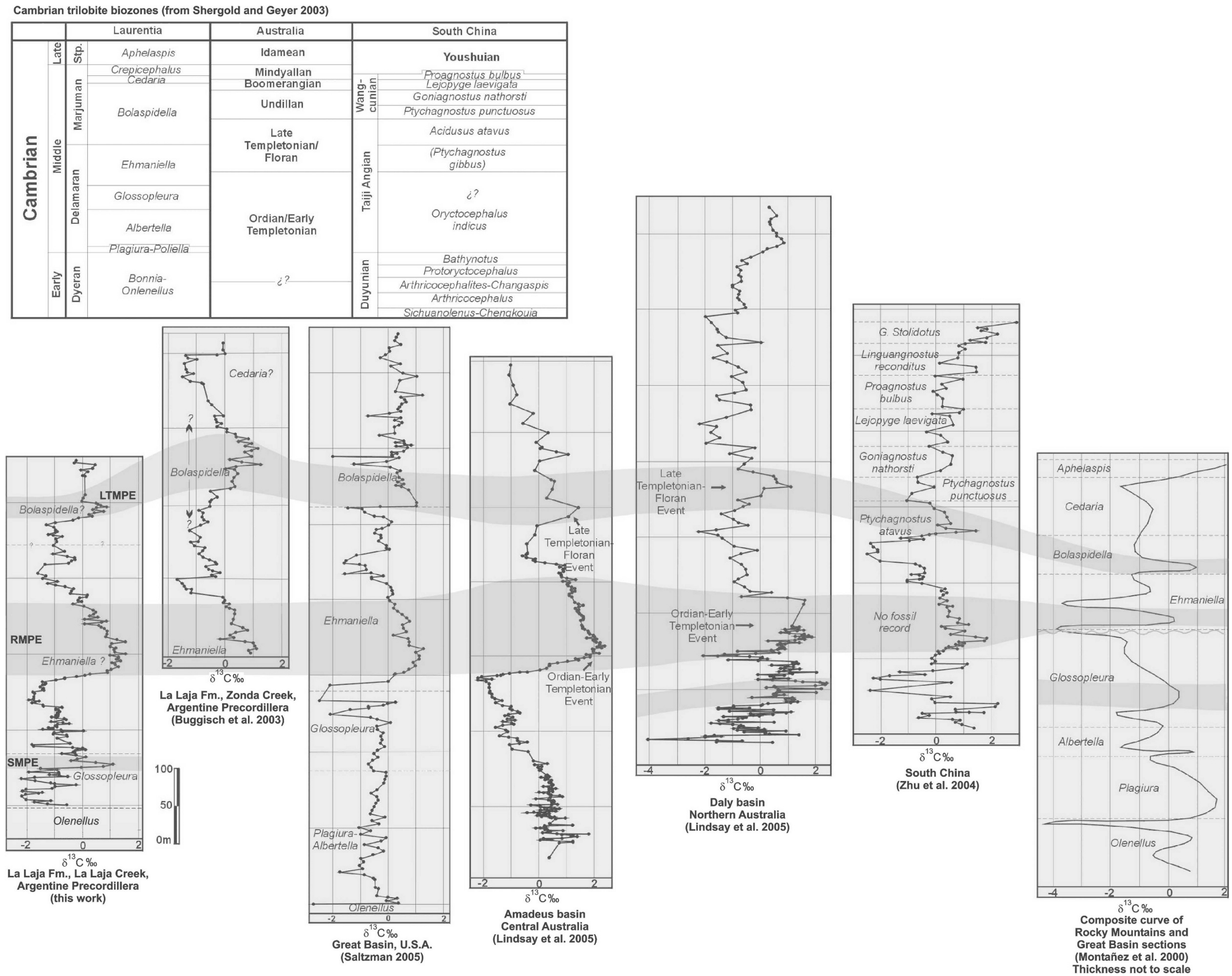

FIG. 7.—Correlation chart between Cambrian C-isotope curves of the Argentine Precordillera (Buggisch et al. 2003 and this work), the Great Basin and Rocky Mountains of U.S.A. (Montañez et al. 2000 and Saltzman 2005), the Amadeus and Daly basins of Australia (Lindsay et al. 2005) and the South China basin (Zhu et al. 2004). Darker bands show excursions discussed in the text. Cambrian trilobite biozones according to Shergold and Geyer (2003). SMPE = Soldano Member Positive Excursion; RMPE = Rivadavia Member Positive Excursion; LTMPE = Las Torres Member Positive Excursion.

could be associated with a relative sea-level fall in a way similar to that proposed for the Rivadavia Member positive excursion. The underlying Juan Pobre siliciclastic section represents relatively deep subtidal deposits and shows negative $\delta^{13}C$ values. This interval would have been deposited during a relative sea-level rise (Gomez and Astini 2006). The Las Torres Member represents very shallow subtidal to intertidal deposits indicating decreasing accommodation space associated with a relative sea-level fall (Gomez and Astini 2006; Gomez et al. 2006) and coincident with the short positive excursion (Fig. 7).

Toward the top of Las Torres Member, the lithofacies do not change significantly but the positive excursion is followed by $\delta^{13}C$ values apparently close to 0‰. The boundary between the La Laja and Zonda formations has been interpreted as a sequence boundary associated with a relative sea-level fall, on the basis of the sharp lithofacies contrast (Gomez and Astini 2006). Although there is no significant change in $\delta^{13}C$ between the La Laja and Zonda formations, there is a sharp decrease in $\delta^{18}O$, which could be interpreted as resulting from meteoric diagenesis at the boundary, although more data are required to confirm this hypothesis. The higher $\delta^{18}O$ values recorded in the lowermost part of the Zonda Formation (Fig. 6) would indicate increasing evaporation under an arid climate associated with the peritidal limestones typical of this unit. Although degradation of microbial mats could have introduced C^{13}-depleted waters during carbonate precipitation (cf. Kah et al. 1999), in peritidal cycles there are no significant differences between the C isotopes recorded in the subtidal and the overlying intertidal and supratidal microbialite-dominated hemicycle (Fig. 6).

CORRELATION WITH OTHER CAMBRIAN CURVES

The $\delta^{13}C$ values of modern oceans range between −0.5‰ and +2‰ (Kroopnick 1985), and, as pointed out by Kaufman and Knoll (1995) and Glumac and Walker (1998), interbasinal correlation of carbon-isotope excursions between 1 and 2‰ is difficult in the absence of sufficient biostratigraphic control. In spite of this, the La Laja $\delta^{13}C$ isotope record shows recognizable isotopic excursions, in some cases varying from −2‰ to +1.6‰ (3.6‰ magnitude of change; Figs. 5, 7). Because of uncertainty in the La Laja Formation biostratigraphy and because there is no detailed documented biostratigraphic information from the La Laja Formation where this study was carried out (La Laja section), our correlation is based mainly on chemostratigraphy.

Three $\delta^{13}C$ positive peaks have been recorded in the La Laja Formation. The magnitude and the highly asymmetrical pattern of these excursions are comparable and easily correlated with available Middle Cambrian curves around the world (Montañez et al. 2000; Zhu et al. 2004; Saltzman 2005; Lindsay et al. 2005). They are also partly recorded in the curve of Buggisch et al. (2003) for the Precordillera basin (Fig. 7).

The similarity and rough synchronicity between these excursions indicate that they are likely related to a perturbation in the global carbon cycle. Similar trends in $\delta^{13}C$ between different sections of the same age are a strong argument for regional or global variations in the carbon isotope composition (Glumac and Walker 1998).

The first $\delta^{13}C$ positive excursion in the lower section of the Soldano Member (*Glossopleura* biozone) seems also present in the Daly Basin (Lindsay et al. 2005), the Rocky Mountains–Great Basin (Montañez et al. 2000) and probably southern China basins (Zhu et al. 2004). The second $\delta^{13}C$ positive excursion, at the Rivadavia Member (Figs. 5, 7), can be partly correlated with that recorded by Buggisch et al. (2003) in a separate section in the Precordillera 13 km to the north and elsewhere (Fig. 7). The third $\delta^{13}C$ positive excursion in the Las Torres Member can also be correlated with a peak in the Zonda section (Fig. 7).

In the $\delta^{13}C$ curve of the Great Basin (Saltzman 2005), two positive excursions were also recorded (Fig. 7). The first one occurs at the boundary between the Chisholm and Dome formations and the second one in the Wheeler Formation. Before the positive excursion of the Dome limestones, shales, siltstones, and mudstones (Palmer 1971b; Sundberg 1991) with a negative isotope signature were recorded in the Chisholm Formation (Saltzman 2005). The boundary between the Chisholm and the Dome coincides with the *Glossopleura–Ehmaniella* biozone boundary (Palmer and Halley 1979; Sundberg 1991). If these positive excursions were correlated, the Rivadavia Member would have been deposited during the *Ehmaniella* biozone. The Wheeler Formation (*Bolaspidella* biozone) positive excursion (Fig. 7) recorded in the data set presented by Saltzman (2005) could be correlated with the $\delta^{13}C$ positive excursion in the equivalent Las Torres Member (Fig. 7).

Comparative analysis between the Precordillera and the Great Basin curves (Fig. 7) in the interval between the *Olenellus* and *Glossopleura* biozones shows some differences in the curve pattern. The Precordillera curve shows a tooth-saw pattern when compared with the uniform Great Basin curve, which has more stable values of $\delta^{13}C$ close to −0.5‰. This difference could be related to the Hawke Bay event that, according to Bordonaro (1999), is present in the Precordillera. Therefore, the *Plagiura–Poliella* and *Albertella* biozones are missing or greatly condensed. Important to note is the fact that this regressive event along the Appalachians has not been recorded in the Great Basin.

Phosphate-rich mudrocks and limestones with low $\delta^{13}C$ values representing starved, transgressive deposits were also recorded at the base of the Giles Creek Dolostone, in the Amadeus Basin (Central Australia) and in the Tindall Limestone in the Daly Basin (Northern Australia), both followed by a sharp positive excursion (Ordian–Early Templetonian Event; Lindsay et al. 2005). The Ordian–Templetonian interval is time equivalent to the lower Middle Cambrian trilobite biozones of Laurentia (Shergold and Geyer 2003) (Fig. 7). Because of this and because the positive excursions are similar (in shape and magnitude) to that recorded in the Rivadavia Member, they could be correlated. Furthermore, as with the Rivadavia positive excursion, the Ordian–Early Templetonian Event recorded within lithofacies deposited during decreasing accommodation space may be associated with a relative sea-level fall. Similarly, the positive peak of the Las Torres Member could be correlated with the Late Templetonian–Floran Event (correlative with the *Ehmaniella–Bolaspidella* interval, Fig. 7) recorded in the Shannon and Jinduckin formations (Amadeus and Daly basins, respectively; Lindsay et al. 2005).

Zhu et al. (2004) also record three positive intervals in the Cambrian of south China (Fig. 7). The first one is recorded in the Qingxudong Formation and the second in the Aoxi Formation limestones following the deposition of ^{13}C-depleted transgressive pyrite-rich black shales. There is no fossil record in the Aoxi Formation, but this unit overlies the Qingxudong Formation, which is considered Early Cambrian in age (Zhu et al. 2004). The third positive excursion is recorded at the base of the Huaqiao Formation (*Ptychagnostus atavus* zone), considered equivalent to the lower *Bolaspidella* biozone (see Shergold and Geyer 2003; Fig. 7). We correlate this with the Las Torres Member positive excursion (Fig. 7).

Similar trends and values were also recorded in the composite curve of Montañez et al. (2000) made from different sections in the Great Basin and the southern Canadian Rockies (Fig. 7). The vertical axis in that curve expresses time, and thickness is not shown. For this reason, and due to the limited chronostratigraphic resolution inherent in trilobite biostratigraphy, accurate correlation between excursions with this curve remains more speculative. Tentatively, the Soldano Member positive excursion could be correlated with the *Glossopleura* biozone $\delta^{13}C$ positive excursion of Montañez et al. (2000) (Fig. 7). The Rivadavia Member positive excursion could be correlated with that of the *Ehmaniella* biozone. The Las Torres Member positive excursion could be correlated with that recorded by Montañez et al. (2000) during the *Bolaspidella* biozone (Fig. 7).

DISCUSSION

A good number of authors (Grotsch et al. 1999; Buggisch et al. 2003; Badenas et al. 2005; among others) commonly interpret $\delta^{13}C$ positive excursions as due to the expansion of the shallow marine realm during sea-level rises. This would produce the broadening of the productive area, increasing organic productivity, and hence enhancing isotope fractionation. In spite of this, and as we discuss in this section, our data need an alternative explanation for the $\delta^{13}C$ positive excursions because according to the facies analysis they seem to be related to decreasing accommodation space during late-stage highstands or sea-level drops. Thus, in our case the "sea-level rise–positive excursion-model" may not apply.

The coincidence of a relative sea-level fall and positive $\delta^{13}C$ excursion could indicate increased burial of C_{org} (organic carbon) due to high organic productivity associated with high riverine (and nutrient) influx to the ocean in a way similar to that proposed by Chen et al. (2002), Weissert et al. (1998), and Glumac and Walker (1998). $\delta^{13}C$ excursions have also been recorded associated with extinctions of trilobite groups and biomere boundaries, and linked to changes in the oceanographic conditions induced by sea-level changes (Palmer 1998; Saltzman et al. 1995; Montañez et al. 2000; Zhu et al. 2004). Saltzman et al. (2000) associated positive $\delta^{13}C$ excursions (SPICE) with a glacio-eustatic sea-level drop enhancing coastal upwelling and triggering benthic extinctions. In fact, the Middle Cambrian positive excursion of Saltzman (2005) coincides with the boundary between the Chisholm and Dome formations (see Data Archive of Saltzman 2005), and Sundberg (1991) placed this boundary coincident with the *Glossopleura–Ehmaniella* limit, where a relative sea-level fall was also documented. High $^{87}Sr/^{86}Sr$ isotope ratios during the Cambrian have been associated with an increased siliciclastic influx from cratonic areas after the Late Proterozoic–Cambrian Pan-African Orogeny (Montañez et al. 1996; Montañez et al. 2000; McArthur et al. 2001). Furthermore, the increasing trend of $^{87}Sr/^{86}Sr$ ratios through the Precambrian–Cambrian boundary has some parallels with increased sediment flux (Flöegel et al. 2000; Hay et al. 2001; McArthur et al. 2001). As proposed by GEOCARB III modeling (Berner and Kothavala 2001), the Early Paleozoic would have been times with very high levels of pCO_2 (15–25 times higher than present). Furthermore, huge first-cycle quartz arenite bodies (15,000,000 km^3) and clay deposits of northern Gondwana have been associated with intense chemical weathering in times of greenhouse climate, with high pCO_2 and $^{87}Sr/^{86}Sr$ isotope ratios following the Pan-African Orogeny in the Cambro-Ordovician (Avigad et al. 2005). During the Cambrian–Ordovician, the development of large-scale mixed carbonates–siliciclastic deposits around the world (Grand Cycles; Aitken 1978; Palmer 1971b; Palmer and Halley 1979; Chow and James 1987; Koerschner and Read 1989; Srinivasan and Walker 1993; Cowan and James 1993; Spencer and Demicco 2002; among others), support the interpretation of availability of siliciclastics, the potential high nutrient flux, and associated increased primary productivity. Relative sea level could have been the main factor controlling the terrigenous distribution and hence the nutrient influx into the ocean. The influx into the ocean of phosphorus (a bio-limiting nutrient) due to selective apatite weathering (Lenton and Watson 2004) is controlled by the activation energy of dissolution, the global temperature, and the surface area of the crystalline rock (Guidry and Mackenzie 2000). The Cambrian, as pointed out earlier, was a greenhouse time (maybe with a quite corrosive atmosphere due to high pCO_2), and crystalline-rock surface area is in fact strongly controlled by relative sea level, so this would have controlled the weathering rates and the nutrient influx into the ocean. Furthermore, the Cambrian is considered to have been a time of sluggish circulation with ocean stratification and a poorly oxygenated deep ocean (Glumac and Walker 1998; Saltzman 2005), and, as previously pointed out, larger values of $\delta^{13}C$ can be driven by high bio-production and increased storage of organic carbon in deep anoxic oceans and sediments. Black shales are also common deposits around the world during the Cambrian (Thickpenny and Leggett 1987; Arthur and Sageman 1994), indicating high preservation of organic matter, maybe due to an expansion of the oxygen-minimum zone and increased organic-carbon burial during increased-productivity cycles. Recent sulfur isotope data of early Templetonian deposits of the Georgina Basin (Australia) are consistent with a significant increase in pyrite burial rates resulting from global anoxia and pyrite formation within the water column (Hough et al. 2006). Of particular interest is a thin interval (0.50 m) of pyrite-rich black shales with phosphatic brachiopods (Pereyra 1985, 1987) overlain by a lenticular body (13.5 m in thickness) of supermature quartz arenites (up to 99 % quartz) and glauconite-rich green shales that have been recorded at the La Cantera section (15 km north of the La Laja section), 9 m below the Soldano–Rivadavia boundary (Astini and Thomas 2000). This section correlates with the fine-grained siliciclastic interval on top of the Soldano Member (La Laja section) recording the negative $\delta^{13}C$ values and followed by the positive excursion at the Rivadavia Member (Gomez and Astini 2006).

Considering the aforementioned, the positive excursion in the Rivadavia Member could be related to high bio-productivity and increased burial of C_{org} produced by high riverine (and nutrient) influx to the ocean associated with a relative sea-level fall. An expansion of the oxygen-minimum zone would also increase the burial of organic carbon enhancing the decoupling of C-isotope signatures between shallow and deep ocean indicated by the positive excursion. A similar interpretation could also be applied to the Las Torres positive excursion.

CONCLUSIONS

Stable-isotope analysis of the Middle Cambrian shallow-marine carbonates of the La Laja Formation (at the La Laja reference section, Argentine Precordillera) record three $\delta^{13}C$ positive excursions. The first excursion occurs in the Soldano Member (*Glossopleura* biozone), the second starts at the base of the Rivadavia Member, and the third occurs during deposition of the Las Torres Member. The upper two excursions are associated with decreasing accommodation space (related to stages of relative sea-level fall) as shown by paleoenvironmental analysis. Similar excursions are roughly coeval with others occurring around the world: Rocky Mountains and the Great Basin (U.S.A.), western Hunan Province (south China), and the Amadeus, Georgina, and Daly basins (Australia). Strong correlations between the $\delta^{13}C$ curves of these different basins suggest a global control in the isotopic signature, although local environmental controls could have partly altered the original isotopic signal. High bio-productivity and increased burial of C_{org} (organic carbon) produced by high riverine (and nutrient) influx to the ocean associated with a relative sea-level fall could provide a mechanism to produce the observed excursions.

Comparative analysis between the La Laja and Great Basin curves in the *Olenellus–Glossopleura* interval is consistent with the existence of either a gap or a condensed section in the Precordillera. This could be interpreted as the record of the Hawke Bay event.

ACKNOWLEDGMENTS

The authors thank Linda C. Kah, Matthew Saltzman, and John Lindsay who read early versions of the manuscript and provided helpful and interesting comments. We also appreciate comments from the Associate Editor (Maya Elrick) and the reviewers Maurice Tucker and Michael Pope that significantly strengthened our interpretations and benefited our work. This research was supported by Consejo Nacional de Investigaciones Científicas y Tecnológicas (PIP 02971/PIP 5783), Agencia Nacional de Ciencia y Tecnología (07–11741) and Secretaría de Ciencia y Tecnología–Universidad Nacional de Córdoba (Resol. 197/05) and an International Association of Sedimentologists student grant to F.J.G. (IAS Grant

Scheme 2005). F.J.G. also thanks Emilia Bertoni and Mateo Martini for fieldwork assistance. Tables A and B are available from JSR's Data Archive, http://www.sepm.org/jsr/jsr_data_archive.asp.

REFERENCES

Aigner, T., 1985, Storm depositional systems: dynamic stratigraphy in modern and ancient shallow-marine sequences: Berlin, Springer-Verlag, Lecture Notes in Earth Sciences, v. 3, 174 p.

Aitken, J.D., 1978, Revised models for depositional Grand Cycles, Cambrian of the Southern Rocky Mountains, Canada: Bulletin of Canadian Petroleum Geology, v. 26, p. 515–542.

Aitken, J.D., 1981, Generalizations about grand cycles, *in* Taylor, M.E., ed., Short Papers for the Second International Symposium of the Cambrian System: U.S. Geological Survey, Open File-Report 81-743, p. 8–14.

Allison, P.A., and Wright, V.P., 2005, Switching off the carbonate factory: A—tidality, stratiphication and brackish wedges in epeiric seas: Sedimentary Geology, v. 179, p. 175–184.

Arthur, M.A., and Sageman, B.B., 1994, Marine black shales: depositional mechanisms and environments of ancient deposits: Annual Review of Earth and Planetary Sciences, v. 22, p. 499–551.

Astini, R.A., 1992, Tectofacies Ordovícicas y evolución de la cuenca eopaleozoica de la Precordillera Argentina: Estudios Geológicos, v. 48, p. 315–327.

Astini, R.A., 1998, Stratigraphical evidence supporting the rifting, drifting and collision of the Laurentian Precordillera terrane of western Argentina, *in* Pankhurst, R.J., and Rapela, C.W., eds., The Proto-Andean margin of Gondwana: Geological Society of London, Special Publication 142, p. 11–33.

Astini, R.A., and Thomas, W.A., 1999, Origin and evolution of the Precordillera terrane of western Argentina: a drifted Laurentian orphan, *in* Ramos, V.A., and Keppie, J.D., eds., Laurentia–Gondwana connections before Pangea: Geological Society of America, Special Paper 336, p. 1–20.

Astini, R.A., and Thomas, W.A., 2000, Quartz-arenites in the Middle Cambrian limestones (La Laja Formation) of the Argentine Precordillera terrane: II Congreso Latinoamericano de Sedimentologia y VIII Reunión Argentina de Sedimentología, Mar del Plata, p. 39–40.

Astini, R.A., and Vaccari, N.E., 1996, Sucesión evaporítica del Cámbrico Inferior de la Precordillera: significado geológico: Asociación Geológica Argentina, Revista, v. 51, p. 97–106.

Astini, R.A., Benedetto, J.L., and Vaccari, N.E., 1995, The early Paleozoic evolution of the Argentine Precordillera as a Laurentian rifted, drifted and collided terrane: a geodynamical model: Geological Society of America, Bulletin, v. 107, p. 253–273.

Astini, R.A., Ramos, V.A., Benedetto, J.L., Vaccari, N.E., and Cañas, F.L., 1996, La Precordillera: Un terreno exótico a Gondwana: XIII Congreso Geológico Argentino y III Congreso de Exploración de Hidrocarburos, Buenos Aires, Actas, 5, p. 293–324.

Avigad, D., Sandler, A., Kolodner, K., Stern, R.J., McWilliams, M., Miller, N., and Beyth, M., 2005, Mass-production of Cambro-Ordovician quartz-rich sandstone as a consequence of chemical weathering of Pan-African terranes: environmental implications: Earth and Planetary Science Letters, v. 240, p. 818–826.

Bádenas, B., Aurell, M., and Gröcke, D.R., 2005, Facies analysis and correlation of high-order sequences in middle–outer ramp successions: variations in exported carbonate on basin-wide $\delta^{13}C_{carb}$ (Kimmeridgian, NE Spain): Sedimentology, v. 52, p. 1253–1275.

Baldis, B.A., and Bordonaro, O.L., 1981, Evolución de facies carbonáticas en la cuenca Cámbrica de la Precordillera de San Juan: VIII Congreso Geológico Argentino, Actas, 2, p. 385–397.

Baldis, B.A., and Bordonaro, O.L., 1984, Cámbrico y Ordovícico en la sierra Chica de Zonda y Cerro Pedernal, Provincia de San Juan. Génesis del margen continental en la Precordillera: IX Congreso Geológico Argentino, San Carlos de Bariloche, Actas, 4, p. 190–207.

Ball, M.M., 1967, Carbonate sand bodies of Florida and the Bahamas: Journal of Sedimentary Petrology, v. 37, p. 556–591.

Banner, J.L., and Hanson, G.N., 1990, Calculation of simultaneous isotopic and trace element variations during water–rock interaction with application to carbonate diagenesis: Geochimica et Cosmochimica Acta, v. 54, p. 3123–3127.

Beeunas, M.A., and Knauth, L.P., 1985, Preserved stable isotopic signature of subaerial diagenesis in the 1.2-b.y. Mezcal Limestone, central Arizona: implications for the timing and development of a terrestrial plant cover: Geological Society of America, Bulletin, v. 96, p. 737–745.

Benedetto, J.L., 2004, The allochthony of the Argentine Precordillera ten years later (1993–2003): a new paleobiogeographic test of the microcontinental model: Gondwana Research, v. 7, p. 1027–1039.

Benedetto, J.L., and Vaccari, N.E., 1992, Significado estratigráfico y tectónico de los complejos de bloques resedimentados Cambro-Ordovícicos de la Precordillera Occidental Argentina: Estudios Geológicos, v. 48, p. 305–313.

Berner, R.A., and Kothavala, Z., 2001, GEOCARB III: A revised model of atmospheric CO_2 over Phanerozoic time: American Journal of Science, v. 301, p. 182–204.

Bordonaro, O.L., 1980, El Cámbrico en la quebrada de Zonda, Provincia de San Juan: Asociación Geológica Argentina, Revista, v. 35, p. 26–40.

Bordonaro, O.L., 1999, Hiatus faunítico (Evento Hawke Bay?) entre el Cámbrico Inferior y Medio en la Formación La Laja, Precordillera de San Juan: XIV Congreso Geológico Argentino, Salta, Actas, 1, 45 p.

Bordonaro, O.L., 2003a, Review of the Cambrian stratigraphy of the Argentine Precordillera: Geológica Acta, v. 1, p. 11–21.

Bordonaro, O.L., 2003b, Evolución paleoambiental y paleogeográfica de la cuenca cámbrica de la Precordillera argentina: Asociación Geológica Argentina, Revista, v. 58, p. 329–346.

Bordonaro, O.L., and Banchig, A., 1996, Estratigrafía de los olistolitos cámbricos de la Precordillera Argentina: XIII Congreso Geológico Argentino, Buenos Aires, Actas, 5, p. 471–479.

Bordonaro, O.L., Beresi, M., and Keller, M., 1993, Reinterpretación estratigráfica del Cámbrico del área de San Isidro, Precordillera de Mendoza: XII Congreso Geológico Argentino, Actas, 2, p. 12–19.

Borrello, A., 1962, Caliza La Laja (Cámbrico Medio, San Juan): Notas Comisión de Investigaciones Científicas de la Provincia de Buenos Aires, La Plata, Argentina, v. 2, p. 3–8.

Borrello, A., 1971, The Cambrian of South America, *in* Holland, C.H., ed., Cambrian of the New World: New York, Wiley Science, Lower Paleozoic Rocks of the World, v. 1, p. 385–438.

Brasier, M.D., and Shukov, S.S., 1998, The falling amplitude of carbon isotopic oscillations through the Lower to Middle Cambrian: northern Siberia data: Canadian Journal of Earth Sciences, v. 35, p. 353–373.

Bridges, P.H., 1972, The significance of tool marks on a Silurian erosional furrow: Geological Magazine, v. 109, p. 405–410.

Buggisch, W., Keller, M., and Lenhert, O., 2003, Carbon isotope record of the Late Cambrian to Early Ordovician carbonates of the Argentina Precordillera: Palaeogeography, Palaeoclimatology, Palaeoecology, v. 195, p. 357–373.

Cañas, F.L., 1995, Early Ordovician carbonate platform facies of the Argentine Precordillera: restricted shelf to open platform evolution, *in* Cooper, J.D., Droser, M.L., and Finney, S.C., eds., Ordovician Odyssey: SEPM, Pacific Section, no. 77, p. 221–224.

Cañas, F.L., 1999, Facies and sequences of the Late Cambrian–Early Ordovician carbonates of the Argentine Precordillera: a stratigraphic comparison with Laurentian platforms, *in* Ramos, V.A., and Keppie, J.D., eds., Laurentia–Gondwana connections before Pangea: Geological Society of America, Special Paper 336, p. 43–62.

Casquet, C., Baldo, E., Pankhurst, R.J., Rapela, C.W., Galindo, C., Fanning, C.M., and Saavedra, J., 2001, Involvement of the Argentine Precordillera terrane in the Famatinian mobile belt: Geochronological (U–Pb Shrimp) and metamorphic evidence from the Sierra de Pie de Palo: Geology, v. 29, p. 703–706.

Cowan, C.A., and James, N.P., 1993, The interactions of sea-level changes, terrigenous-sediment influx and carbonate productivity as controls on Upper Cambrian Grand Cycles of western Newfoundland, Canada: Geological Society of America, Bulletin, v. 105, p. 1576–1590.

Chen, D., Tucker, M.E., Shen, Y., Yans, J., and Preat, A., 2002, Carbon isotope excursions and sea-level change: implications for the Frasnian–Famennian biotic crisis: Geological Society of London, Journal, v. 159, p. 623–626.

Chow, N., and James, N.P., 1987, Cambrian Grand Cycles: a northern Appalachian perspective: Geological Society of America, Bulletin, v. 98, p. 418–429.

Cozzi, A., Allen, P.A., and Grotzinger, J.P., 2004, Understanding carbonate ramp dynamics using $\delta^{13}C$ profiles: examples from the Neoproterozoic Buah Formation of Oman: Terranova, v. 16, p. 62–67.

Demicco, R.V., 1983, Wavy and lenticular-bedded carbonate ribbon rocks of the Upper Cambrian Conococheague limestone, Central Appalachians: Journal of Sedimentary Petrology, v. 54, p. 1121–1132.

Demicco, R.V., and Hardie, L.A., 1994, Sedimentary structures and early diagenetic features of shallow marine carbonate deposits: SEPM, Atlas Series 1, 265 p.

Dott, R.H., Jr., 2003, The importance of eolian abrasion in supermature quartz sandstones and the paradox of weathering on vegetation-free landscapes: Journal of Geology, v. 111, p. 387–405.

Duringer, P., and Vecsei, A., 1998, Middle Triassic shallow water limestones from the Upper Muschelkalk of eastern France: the origin and depositional environment of some early Mesozoic fine-grained limestones: Sedimenatry Geology, v. 121, p. 57–70.

Flögel, S., Wold, C.N., and Hay, W.W., 2000, Evolution of sediments and ocean salinity: 31st International Geological Congress: Rio de Janeiro, Brazil, August 6–17, Abstracts Volume, CD-ROM, 4.

Flügel, E., 1982, Microfacies Analysis of Limestones: Berlin, Springer-Verlag, 633 p.

Flügel, E., 2004, Microfacies of Carbonate Rocks: Analysis, Interpretation and Application: Berlin, Springer-Verlag, 976 p.

Foglia, R.D., and Vaccari, N.E., 2006, La biozona de *Glossopleura* (Delamariano, Cámbrico Medio) en el Miembro Soldano, Formación La Laja, San Juan, Argentina: IX Congreso Argentino de Paleontología y Bioestratigrafía, Córdoba, September 18–22, 2006, p. 158.

Galindo, C., Casquet, C., Rapela, C., Pankhurst, R.J., Baldo, E., and Saavedra, J., 2004, Sr, C and O isotope geochemistry and stratigraphy of Precambrian and Lower Paleozoic carbonate sequences from the Western Sierras Pampeanas of Argentina: tectonic implications: Precambrian Research, v. 131, p. 55–71.

Gao, G., and Land, L.S., 1991, Geochemistry of Cambro-Ordovician Arbuckle Limestone, Oklahoma: implications for diagenetic $\delta^{18}O$ alteration and secular $\delta^{13}C$ and $^{87}Sr/^{86}Sr$ variation: Geochimica et Cosmochimica Acta, v. 55, p. 2911–2920.

Glumac, B., and Walker, K.R., 1998, A Late Cambrian positive carbon-isotope excursion in the Southern Appalachians: relation to biostratigraphy, sequence stratigraphy, environments of deposition, and diagenesis: Journal of Sedimentary Research, v. 68, p. 1212–1222.

Gomez, F.J., and Astini, R.A., 2004, Rudstones intraclásticos inusuales en el Cámbrico de la Precordillera: posible origen y significado paleoambiental: Reunión Argentina de Sedimentología, San Luis, Actas, 1, p. 75–77.

Gomez, F.J., and Astini, R.A., 2005, Cianobacterias renalciformes en el Cámbrico Medio de la Precordillera Argentina: morfología, posición estratigráfica y significado paleoambiental: Ameghiniana, v. 42, p. 221–232.

Gomez, F.J., and Astini, R.A., 2006, Sedimentología y paleoambientes de la Formación La Laja (Cámbrico), Quebrada La Laja, Sierra Chica de Zonda, San Juan, Argentina: Revista Geológica de Chile, v. 33, p. 19–46.

Gomez, F.J., Martini, M., and Astini, R.A., 2006, Ciclos perimareales y estructuras microbialiticas en el Miembro Las Torres, extremo norte de la Sierra Chica de Zonda, San Juan, Argentina: IV Congreso Latinoamericano de Sedimentología y XI Reunión Argentina de Sedimentología, San Carlos de Bariloche, Argentina.

Grötsch, J., Billing, I., and Vahrenkamp, V., 1999, Carbon-isotope stratigraphy in shallow-water carbonates: implications for Cretaceous black-shale deposition. Sedimentology, v. 45, p. 623–634.

Guidry, M.W., and Mackenzie, F.T., 2000, Apatite weathering and the Phanerozoic phosphorus cycle: Geology, v. 28, p. 631–634.

Gutzmer, J., and Beukas, N.J., 1998, Earliest laterites and possible evidence for terrestrial vegetation in the Early Proterozoic: Geology, v. 26, p. 263–266.

Hardie, L.A., 1986, Stratigraphic models for carbonate tidal flat deposition, *in* Hardie, L.A., and Shinn, E.A., eds., Carbonate Depositional Environments, Modern and Ancient, Part 3, Colorado School of Mines, v. 81, p. 59–74.

Hay, W.W., Wold, C.N., Soeding, E., and Flögel, S., 2001, Evolution of sediment fluxes and ocean salinity, *in* Merriam, D.F., and Davis, J.C., eds., Geologic Modeling and Simulation: Sedimentary Systems: New York, Kluwer Academic/Plenum Publishers, p. 153–167.

Holmden, C., Creaser, R.A., Muehlenbachs, K., Leslie, S.A., and Bergström, S.M., 1998, Isotopic evidence for geochemical decoupling between ancient epeiric seas and bordering oceans: implications for secular curves: Geology, v. 26, p. 567–570.

Horodyski, R.J., and Knauth, L.P., 1994, Life on land in the Precambrian: Science, v. 263, p. 494–498.

Hough, M.L., Shields, G.A., Evins, L.Z., Strauss, H., Henderson, R.A., and Mackenzie, S., 2006, A major sulphur isotope event at c. 510 Ma: a possible anoxia–extinction–volcanism connection during Early–Middle Cambrian transition?: Terra Nova, v. 18, p. 257–263.

Huff, W.D., Bergström, S.M., Kolata, D.R., Cingolani, C.A., and Astini, R.A., 1998, Ordovician K-bentonites in the Argentine Precordllera: relations to Gondwana margin evolution, *in* Pankhurst, R.J., and Rapela, C.W., eds., The Proto-Andean Margin of Gondwana: Geological Society of London, Special Publication 142, p. 107–126.

James, N.P., Stevens, R.K., Barnes, C.R., and Knight, I., 1989, Evolution of a Lower Paleozoic continental-margin carbonate platform, northern Canadian Appalachians, *in* Crevello, P.D., Wilson, J.L., Sarg, J.F., and Read, J.F., eds., Controls on Carbonate Platform and Basin Development: SEPM, Special Publication 44, p. 123–146.

Kah, L.C., Sherman, A.G., Narbonne, G.M., Knoll, A.H., and Kaufman, A.J., 1999, $\delta^{13}C$ stratigraphy of the Proterozoic Bylot Supergroup, Baffin Island, Canada: Implications for regional lithostratigraphic correlations: Canadian Journal of Earth Sciences, v. 36, p. 313–332.

Kaufman, A.J., and Knoll, A.H., 1995, Neoproterozoic variations in the C-isotopic composition of seawater: stratigraphic and biogeochemical implications: Precambrian Research, v. 73, p. 27–49.

Kay, S.M., Orrel, S., and Abbruzzi, J.M., 1996, Zircon and whole rock Nd–Pb isotopic evidence for a Grenville age and Laurentian origin for the basement of the Precordillera terrane in Argentina: Journal of Geology, v. 104, p. 637–648.

Keller, M., 1999, Argentine Precordillera: Sedimentary and Plate Tectonic History of a Laurentian Crustal Fragment in South America: Geological Society of America, Special Paper 431, 131 p.

Keller, M., Cañas, F., Lehnert, O., and Vaccari, N.E., 1994, The Upper Cambrian and Lower Ordovician of the Precordillera (Western Argentina): Some stratigraphic reconsiderations: Newsletters on Stratigraphy, v. 31, p. 115–132.

Keller, M., Buggisch, W., and Lehnert, O., 1998, The stratigraphic record of the Argentine Precordillera and its plate tectonic background, *in* Pankhurst, R.J., and Rapela, C.W., eds., Proto-Andean margin of Gondwana: Geological Society of London, Special Publication 142, p. 35–56.

Koerschner, W.F., and Read, J.F., 1989, Field and modelling studies of Cambrian carbonate cycles, Virginia Appalachians: Journal of Sedimentary Petrology, v. 59, p. 654–687.

Kozar, M.G., Weber, L.J., and Walker, K.R., 1990, Field and modelling studies of Cambrian carbonate cycles, Virginia Appalachians—Discussion and Reply: Journal of Sedimentary Petrology, v. 60, p. 790–796.

Kreisa, R.D., 1981, Storm-generated sedimentary structures in subtidal marine facies with examples from the Middle and Upper Ordovician of southwestern Virginia: Journal of Sedimentary Petrology, v. 51, p. 823–848.

Kroopnick, P.M., 1985, The distribution of ^{13}C of ΣCO_2 in the world ocean: Deep-Sea Research, v. 32, p. 57–84.

Kump, L.R., 1991, Interpreting carbon-isotope excursions: Strangelove oceans: Geology, v. 19, p. 299–302.

Kump, L.R., and Arthur, M.A., 1999, Interpreting carbon-isotope excursions: carbonates and organic matter: Chemical Geology, v. 161, p. 181–198.

Lenton, T.M., and Watson, A.J., 2004, Biotic enhancement of weathering, atmospheric oxygen and carbon dioxide in the Neoproterozoic: Geophysical Research Letters, v. 31, L05202, 10.1029/2003GL018802.

Lindsay, J.F., Kruse, P.D., Green, O.R., Hawkins, E., Brasier, M.D., Cartlidge, J., and Corfield, R.M., 2005, The Neoproterozoic–Cambrian record in Australia: a stable isotope study: Precambrian Research, v. 143, p. 113–133.

Lukasik, J.J., James, N.P., McGowran, B., and Bone, Y., 2000, An epeiric ramp: low energy, cool-water carbonate facies in a Tertiary inland sea, Murray Basin, South Australia: Sedimentology, v. 47, p. 851–881.

McArthur, J.M., Howarth, R.J., and Bailey, T.R., 2001, Strontium isotope stratigraphy: LOWES Version 3: Best fit to the marine Sr-isotope curve for 0–509 Ma and accompanying look-up table for deriving numerical age: Journal of Geology, v. 109, p. 155–170.

McKerrow, W.S., Scotese, C.R., and Brasier, M.D., 1992, Early Cambrian continental reconstructions: Geological Society of London, Journal, v. 149, p. 559–606.

Meng, X., Ge, M., and Tucker, M.E., 1997, Sequence stratigraphy, sea level changes and depositional systems in the Cambro-Ordovician of the North China carbonate platform: Sedimentary Geology, v. 114, p. 189–222.

Montañez, I.P., Banner, J.L., Osleger, D.A., Borg, L.E., and Bosserman, P.J., 1996, Integrated Sr isotope variations and sea-level history of Middle to Upper Cambrian platform carbonates: Implications for the evolution of Cambrian seawater $^{87}Sr/^{86}Sr$: Geology, v. 24, p. 917–920.

Montañez, I.P., Osleger, D.A., Banner, J.L., Mack, L.E., and Musgrove, M., 2000, Evolution of the Sr and C isotope composition of Cambrian oceans: GSA Today, v. 10, p. 1–7.

Mount, J.F., 1984, Mixing of siliciclastic and carbonate sediments in shallow shelf environments: Geology, v. 12, p. 432–435.

Myrow, P.M., 1992, Pot and gutter casts from the Chapel Island Formation, southeast Newfoundland: Journal of Sedimentary Petrology, v. 62, p. 999–1007.

Myrow, P.M., 1994, Pot and gutter casts from the Chapel Island Formation, southeast Newfoundland—Reply: Journal of Sedimentary Research, v. 62, p. 708–709.

Naipauer, M., Cingolani, C.A., Valencio, S., Chemale, F., and Vujovich, G.I., 2005, Estudios isotopicos en carbonatos marinos del terreno Precordillera–Cuyania: ¿Plataforma común en el Neoproterozoico–Paleozoico Inferior? Latin American Journal of Sedimentology and Basin Analysis, v. 12, p. 89–108.

Odin, G.S., and Matter, A., 1981, De glauconiarum origine: Sedimentology, v. 28, p. 611–641.

Osleger, D., 1991, Subtidal carbonate cycles: implications for allocyclic vs. autocyclic controls: Geology, v. 19, p. 917–920.

Osleger, D., and Read, J.F., 1991, Relation of eustasy to stacking patterns of meter-scale carbonate cycles, Late Cambrian, U.S.A.: Journal of Sedimentary Petrology, v. 61, p. 1225–1252.

Palmer, A.R., 1971a, The Cambrian of the Appalachian and Eastern New England regions, Eastern United States, *in* Holland, E.R., ed., Cambrian of the New World: New York, Wiley Interscience, p. 169–217.

Palmer, A.R., 1971b, The Cambrian of the Great Basin, Western United States, *in* Holland, E.R., ed., Cambrian of the New World: New York, Wiley Interscience, p. 1–78.

Palmer, A.R., 1998, A proposed nomenclature for stages and series for the Cambrian of Laurentia: Canadian Journal of Earth Sciences, v. 35, p. 323–328.

Palmer, A.R., and Halley, R.B., 1979, Physical stratigraphy and trilobite biostratigraphy of the Carrara Formation (Lower and Middle Cambrian) of the southern Great Basin: U.S. Geological Survey, Professional Paper 1047, 131 p.

Palmer, A.R., and James, N.P., 1979, The Hawke Bay Event: a circum Iapetus regression event near the Lower–Middle Cambrian boundary: Proceedings of the International Geological Correlation Project Meetings, p. 15–18.

Panchuk, K.M., Holmden, C.E., and Kump, L.R., 2005, Sensitivity of epeiric sea carbon isotope record to local-scale carbon cycle processes: tales from the Mohawkian Sea: Palaeogeography, Palaeoclimatology, Palaeoecology, v. 228, p. 320–337.

Panchuk, K.M., Holmden, C.E., and Leslie, S.A., 2006, Local controls on carbon cycling in the Ordovician Midcontinent region of North America, with implications for carbon isotope secular curves: Journal of Sedimentary Research, v. 76, p. 200–211.

Patterson, W.P., and Walter, L.M., 1994, Depletion of ^{13}C in seawater ΣCO_2 on modern carbonate platforms: significance for the carbon isotopic record of carbonates: Geology, v. 22, p. 885–888.

Pelechaty, S.M., Kaufman, A.J., and Grotzinger, J.P., 1996, Evaluation of $\delta^{13}C$ chemostratigraphy for intrabasinal correlation: Vendian strata of northeast Siberia: Geological Society of America, Bulletin, v. 108, p. 992–1003.

Pereyra, B.R., 1985, Análisis estratigráfico y genético de los niveles cámbricos del C° de Zonda, provincia de San Juan: Primeras Jornadas de Precordillera, San Juan, Acta, 1, p. 24–29.

Pereyra, B.R., 1987, Niveles carbonoso–psammiticos cámbricos en el Cerro de Zonda, Provincia de San Juan: X Congreso Geológico Argentino, San Miguel de Tucuman, Actas, 3, p. 61–64.

Peryt, T.M., 1983, Oncoids: Comment to recent developments, *in* Peryt, T.M., ed., Coated Grains: Berlin, Springer-Verlag, p. 273–275.

Pratt, B.R., and James, N.P., 1986, The St George Group (Lower Ordovician) of western Newfoundland: tidal flat island model for carbonate sedimentation in shallow epeiric seas: Sedimentology, v. 33, p. 313–343.

Prave, A.R., 2002, Life on land in the Proterozoic: evidence from Torridonian rocks of northwest Scotland: Geology, v. 30, p. 811–814.

Ramos, V.A., Jordan, T.E., Allmendinger, R.W., Mpodozis, C., Kay, S.M., Cortés, J.M., and Palma, M.A., 1986, Paleozoic terranes of the central Argentine–Chilean Andes: Tectonics, v. 5, p. 855–880.

Rankey, E.C., Walker, K., and Srinivasan, K., 1994, Gradual establishment of Iapetan "passive" margin sedimentation: Stratigraphic consequences of Cambrian episodic tectonism and eustasy, southern Appalachians: Journal of Sedimentary Research, v. 64, p. 298–310.

Rapalini, A.E., and Astini, R.A., 1998, Paleomagnetic confirmation of the allochthony of the Argentine Precordillera: Earth and Planetary Science Letters, v. 155, p. 1–14.

Read, J.F., 1989, Evolution of Cambro-Ordovician passive margin, U.S. Appalachians, *in* Rankin, D.W., Drake, A.A., Glover, L., Goldsmith, R., Hall, L.M., Murray, D.P., Ratcliffe, N.M., Read, J.F., Secor, D.T., and Stanley, R.S., eds., Pre-orogenic terranes: Geological Society of America, The Geology of North America, v. F-2, The Appalachian–Ouachita Orogen in the United States, p. 42–57.

Saltzman, M.R., 2005, Phosphorus, nitrogen, and the redox evolution of the Paleozoic oceans: Geology, v. 33, p. 573–576.

Saltzman, M.R., Davidson, J.P., Holden, P., and Lohmann, K.C., 1995, Sea-level driven changes in ocean chemistry at Upper Cambrian extinction horizon: Geology, v. 23, p. 893–896.

Saltzman, M.R., Ripperdan, R.L., Brasier, M.D., Lohmann, K.C., Robison, R.A., Chang, W.T., Peng, S., Ergaliev, E.K., and Runnegar, B., 2000, A global carbon isotope excursion (SPICE) during the Late Cambrian: relation to trilobite extinctions, organic-matter burial and sea-level: Palaeogeography, Palaeoclimatology, Palaeoecology, v. 162, p. 211–223.

Scotese, C.R., Boucot, A.J., and McKerrow, W.S., 1999, Gondwanan palaeogeography and paleoclimatology: Journal of African Earth Sciences, v. 28, p. 99–114.

Shergold, J.H., and Geyer, G., 2003, The Subcommission on Cambrian Stratigraphy: the status quo: Geologica acta, v. 1, p. 5–9.

Sial, A.N., Ferreira, V.P., Toselli, A.J., Aceñolaza, F.G., Pimentel, M.M., Parada, M.A., and Alonso, R.N., 2001, C and Sr isotopic evolution of carbonate sequences in NW Argentina: Implications for a probable Precambrian–Cambrian transition: Carbonates and Evaporites, v. 16, p. 141–152.

Sial, A.N., Peralta, S., Ferreira, V.P., Toselli, A.J., Aceñolaza, F.G., Parada, M.A., Gaucher, C., Alonso, R.N., and Pimentel, M.M., 2003, C–O–Sr-isotope chemostratigraphy of Cambrian carbonates sequences, Precordillera, western Argentina: IV South American Symposium on Isotope Geology, Abstracts, p. 390–393.

Sloss, L.L., 1963, Sequences in the cratonic interior of North America: Geological Society of America, Bulletin, v. 74, p. 93–114.

Spencer, R.J., and Demicco, R.V., 2002, Facies and sequence stratigraphy of two Cambrian Grand Cycles: implications for Cambrian sea level and orogin of Grand Cycles: Bulletin of Canadian Petroleum Geology, v. 50, p. 478–491.

Srinivasan, K., 1993, Depositional history, sequence stratigraphy and diagenesis of Maryville limestone (Middle Cambrian), Southern Appalachians [PhD Thesis]: University of Tennessee, Knoxville, 165 p.

Srinivasan, K., and Walker, K., 1993, Sequence stratigraphy of an intrashelf basin carbonate ramp to rimmed platform transition: Maryville Limestone (Middle Cambrian), southern Appalachians: Geological Society of America, Bulletin, v. 105, p. 883–896.

Sundberg, F.A., 1991, Paleogeography of western Utah and Eastern Nevada during the Ehmaniella Biochron (Middle Cambrian), *in* Cooper, J.D., and Stevens, C.H., eds., Paleozoic Paleogeography of the Western United States—II: SEPM, Pacific Section, v. 67, p. 387–399.

Thickpenny, A., and Leggett, J.K., 1987, Stratigraphic distribution and palaeo-oceanographic significance of European early Paleozoic organic-rich sediments, *in* Brooks, J., and Fleet, A.J., eds., Marine Petroleum Source Rocks: Geological Society of London, Special Publication 26, p. 231–247.

Thomas, W.A., and Astini, R.A., 1996, The Argentine Precordillera; a traveler from the Ouachita Embayment of North America Laurentia: Science, v. 273, p. 752–757.

Thomas, W.A., and Astini, R.A., 1999, Simple-shear conjugate rift margins of the Argentine Precordillera and the Ouachita embayment of Laurentia: Geological Society of America, Bulletin, v. 111, p. 1069–1079.

Thomas, W.A., and Astini, R.A., 2003, Ordovician accretion of the Argentine Precordillera terrane to Gondwana: a review: Journal of South American Earth Sciences, v. 16, p. 67–79.

Thomas, W.A., Astini, R.A., and Denison, R.E., 2001, Strontium isotopes, age, and tectonic setting of Cambrian salinas along the rift and transform margins of the Argentine Precordillera and Southern Laurentia: Journal of Geology, v. 109, p. 231–246.

Thomas, W.A., Astini, R.A., Mueller, P.A., Gehrels, G.E., and Wooden, J.L., 2004, Transfer of the Argentine Precordillera terrane from Laurentia: constraints from detrital-zircon geochronology: Geology, v. 32, p. 965–968.

Tucker, M.E., and Wright, V.P., 1990, Carbonate Sedimentology, Oxford, U.K., Blackwell Science, 482 p.

Vaccari, N.E., 1994, Las faunas de trilobites de las sucesiones carbonáticas del Cámbrico y Ordovícico temprano de la Precordillera septentrional, República Argentina [Tesis Doctoral]: Universidad Nacional de Córdoba, Córdoba, 271 p.

Vahrenkamp, V.C., and Rossinsky, V., 1987, Preserved stable isotopic signature of subaerial diagenesis in the Mezcal Limestone, Central Arizona: implications for the timing of a terrestrial plant cover—Discussion and Reply: Geological Society of America, Bulletin, v. 99, p. 595–597.

Watanabe, Y., Martini, J.E.J., and Ohmoto, H., 2000, Geochemical evidence for terrestrial ecosystems 2.6 billion years ago: Nature, v. 408, p. 574–578.

Weissert, H., Lini, A., Föllmi, K.B., and Kuhn, O., 1998, Correlation of Early Cretaceous carbon isotope stratigraphy and platform drowning events: a possible link? Palaeogeography, Palaoclimatology, Palaeoecology, v. 137, p. 189–203.

Wells, M.R., Allison, P.A., Hampson, G.J., Piggott, M.D., and Pain, C.C., 2005, Modelling ancient tides: the Upper Carboniferous epi-continental seaway of Northwest Europe: Sedimentology, v. 52, p. 715–735.

Wright, V.P., and Burchette, T.P., 1996, Shallow-water carbonate environments, *in* Reading, H.G., ed., Sedimentary Environments; Proccesses, Facies and Stratigraphy: Oxford, U.K., Blackwell Science, p. 325–394.

Zhu, M.Y., Zhang, J.M., Li, G.X., and Yang, A.H., 2004, Evolution of C isotopes in the Cambrian of China: implications for Cambrian subdivision and trilobite mass extinctions, Géobios, v. 37, p. 287–301.

Received 27 September 2006; accepted 4 March 2007.